

AD-A055 856

AIR FORCE INST OF TECH WRIGHT-PATTERSON AFB OHIO SCH--ETC F/G 11/6
DETERMINATION OF THRESHOLD STRESS INTENSITY FACTORS FOR 7175-T6--ETC(U)
SEP 77 D R HOLLOWAY

UNCLASSIFIED

AFIT/GAE-MC/77S-1

NL

OF
ADA
065856



END

DATE
FILMED

8 -78

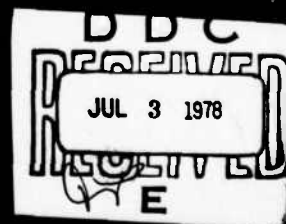
DDC

ADA
558

AD No. _____

DDC FILE COPY

AD A 055856



AD A 055856

①

AD No. _____

DDC FILE COPY

⑥

DETERMINATION OF THRESHOLD STRESS
INTENSITY FACTORS FOR 7175-T651 ALUMINUM
AND ALCOA MA-87 POWDERED ALUMINUM ALLOYS.

⑨ Master's THESIS,

④

AFIT/GAE/MC/77S-1

⑩

Donald R. Holloway
Captain USAF

⑪ Sep 77

⑬ 2307

⑫ 68p.

⑭ P1

DDC
RECEIVED
JUL 3 1978
RECEIVED

OK

E

Approved for Public Release; Distribution Unlimited.

78 06 30 021

012 225

CL

AFIT/GAE/MC/77S-1

DETERMINATION OF THRESHOLD STRESS INTENSITY FACTORS FOR
7175-T651 ALUMINUM AND ALCOA MA-87 POWDERED ALUMINUM ALLOYS

THESIS

Presented to the Faculty of the School of Engineering
of the Air Force Institute of Technology

Air University

in Partial Fulfillment of the
Requirements for the Degree of
Master of Science

by

ACCESSION for	
NTIS	White Section <input checked="" type="checkbox"/>
DDC	Buff Section <input type="checkbox"/>
UNANNOUNCED	<input type="checkbox"/>
JUSTIFICATION	
BY	
DISTRIBUTION/AVAILABILITY CODES	
Dist.	AVAIL. and/or SPECIAL
A	

Donald R. Holloway, B.S.A.E.
Captain USAF

Graduate Aeronautical Engineering

September 1977

Approved for public release; distribution unlimited.

PREFACE

This study was undertaken to continue investigation of an Air Force research problem. This problem was to determine threshold stress intensity factors for two aluminum alloys: 7175-T651 and a new powdered alloy, Alcoa MA-87.

The research was performed in the materials testing laboratory, Air Force Institute of Technology, Wright-Patterson Air Force Base, Ohio. I am indebted to Dr. Dennis Corbly of the Air Force Materials Laboratory for his assistance, guidance and sponsorship. I wish to thank Dr. Peter Torvik for the direction and support given to me in his capacity as my thesis advisor. I would also like to thank Dr. Richard E. Johnson for his advice on performing the tests.

Donald R. Holloway

TABLE OF CONTENTS

	<u>Page</u>
Preface.	ii
List of Figures.	iv
List of Tables	vii
Abstract	viii
I. INTRODUCTION	1
Background	1
Literature Survey.	2
Problem Definition	6
II. MATERIALS.	7
III. EXPERIMENTAL PROCEDURE	10
Test Apparatus	10
Specimen Configuration	12
Specimen Preparation	12
Testing.	12
Crack Measurement.	16
Post-test Measurement.	16
Data Reduction	19
IV. RESULTS AND DISCUSSION	22
V. CONCLUSIONS AND RECOMMENDATIONS.	27
Conclusions	27
Recommendations	27
Bibliography.	28
Appendix A	
Supplementary Data.	30
Vita.	56

LIST OF FIGURES

<u>Figure</u>		<u>Page</u>
1	Schematic Illustration of the Fatigue Crack Growth Rate as a Function of Stress Intensity Range. . . .	3
2	Dimensionless Proportionality Factors for Edge-Cracked Bend Specimen.	5
3	Schematic of Sonntag Universal Fatigue Testing Machine.	11
4	Edge-Cracked Bend Specimen	13
5	L-T (Longitudinal-Transverse) Specimen	14
6	T-L (Transverse-Longitudinal) Specimen	14
7	Average Crack Length Versus $\Delta P (\Delta P = P_{\max} - P_{\min})$ for Specimen #7 (7175-T651 L-T, R = 0.1)	15
8	Sonntag Universal Fatigue Testing Machine.	17
9	Edge-Cracked Bend Specimen Mounted in Sonntag Universal Fatigue Testing Machine.	18
10	7175-T651 Fracture Surface (Divisions in 1/64 inch). . . .	20
11	Alcoa MA-87 Fracture Surface (Divisions in 1/64 inch). . .	20
12	Average Crack Length Versus Number of Cycles for Specimen #7 (7175-T651 L-T, R = 0.1)	23
13	Fatigue Crack Growth Rate Versus Stress Intensity Factor Range for Specimen #7 (7175-T651 L-T, R = 0.1). . .	24
14	Threshold Stress Intensity Factors Versus Stress Ratio . .	26
15	Average Crack Length Versus $\Delta P (\Delta P = P_{\max} - P_{\min})$ for Specimen #1 (7175-T651 T-L, R = 0.1)	32
16	Average Crack Length Versus Number of Cycles for Specimen #1 (7175-T651 T-L, R = 0.1)	33
17	Fatigue Crack Growth Rate Versus Stress Intensity Factor Range for Specimen #1 (7175-T651 T-L, R = 0.1). . .	34
18	Average Crack Length Versus $\Delta P (\Delta P = P_{\max} - P_{\min})$ for Specimen #6 (7175-T651 L-T, R = 0.1)	35

LIST OF FIGURES (cont'd)

<u>Figure</u>		<u>Page</u>
19	Average Crack Length Versus Number of Cycles for Specimen #6 (7175-T651 L-T, R = 0.1).	36
20	Fatigue Crack Growth Rate Versus Stress Intensity Factor Range for Specimen #6 (7175-T651 L-T, R = 0.1) . .	37
21	Average Crack Length Versus $\Delta P(\Delta P = P_{\max} - P_{\min})$ for Specimen #8 (7175-T651 L-T, R = 0.1).	38
22	Average Crack Length Versus Number of Cycles for Specimen #8 (7175-T651 L-T, R = 0.1).	39
23	Fatigue Crack Growth Rate Versus Stress Intensity Factor Range for Specimen #8 (7175-T651 L-T, R = 0.1) . .	40
24	Average Crack Length Versus $\Delta P(\Delta P = P_{\max} - P_{\min})$ for Specimen #9 (7175-T651 L-T, R = 0.3).	41
25	Average Crack Length Versus Number of Cycles for Specimen #9 (7175-T651 L-T, R = 0.3).	42
26	Fatigue Crack Growth Rate Versus Stress Intensity Factor Range for Specimen #9 (7175-T651 L-T, R = 0.3) . .	43
27	Average Crack Length Versus $\Delta P(\Delta P = P_{\max} - P_{\min})$ for Specimen #10 (7175-T651 L-T, R = 0.3)	44
28	Average Crack Length Versus Number of Cycles for Specimen #10 (7175-T651 L-T, R = 0.3)	45
29	Fatigue Crack Growth Rate Versus Stress Intensity Factor Range for Specimen #10 (7175-T651 L-T, R = 0.3). .	46
30	Average Crack Length Versus $\Delta P(\Delta P = P_{\max} - P_{\min})$ for Specimen #13 (MA-87 T-L, R = 0.1)	47
31	Average Crack Length Versus Number of Cycles for Specimen #13 (MA-87 T-L, R = 0.1)	48
32	Fatigue Crack Growth Rate Versus Stress Intensity Factor Range for Specimen #13 (MA-87 T-L, (R = 0.1) . . .	49
33	Average Crack Length Versus $\Delta P(\Delta P = P_{\max} - P_{\min})$ for Specimen #15 (MA-87 T-L, R = 0.1)	50
34	Average Crack Length Versus Number of Cycles for Specimen #13 (MA-87 T-L, R = 0.1)	51

LIST OF FIGURES (cont'd)

<u>Figure</u>		<u>Page</u>
35	Fatigue Crack Growth Rate Versus Stress Intensity Factor Range for Specimen #15. (MA-87 T-L, R = 0.1). . . .	52
36	Average Crack Length Versus $\Delta P (\Delta P = P_{\max} - P_{\min})$ for Specimen #16 (MA-87 T-L, R = 0.3)	53
37	Average Crack Length Versus Number of Cycles for Specimen #16 (MA-87 T-L, R = 0.3)	54
38	Fatigue Crack Growth Rate Versus Stress Intensity Factor Range for Specimen #16 (MA-87 T-L, R = 0.3). . . .	55

LIST OF TABLES

<u>Table</u>		<u>Page</u>
I	Chemical Composition (Weight Percent) of 7175-T651 and MA-87 Aluminum Alloys.	7
II	Mechanical Properties of 7175-T651 and MA-87 Aluminum Alloys.	8
III	Heat Treatment and Aging Process of 7175-T651 Aluminum Alloy	8
IV	Heat Treatment and Aging Process of MA-87 Aluminum Alloy	9
V	Comparison of Visual and Post-Test Crack Measurements. .	21
VI	Threshold Stress Intensity Factor Tests (ΔK_{TH} in KSI $\sqrt{IN.}$)	25

ABSTRACT

Threshold stress intensity factors were obtained for two aluminum alloys: 7175-T651 and Alcoa MA-87, a powdered alloy. Crack growth tests were conducted at room temperature on a Sonntag Universal fatigue testing machine. Edge-cracked bend specimens were used in the tests. Crack length was checked periodically using a Gaertner cathetometer coupled with an auxillary lens placed close to the specimen. Tests were performed at stress ratios of $R = 0.1$ and $R = 0.3$. It was found that 7175-T651 had a greater fatigue threshold value than MA-87 when compared at the same stress ratio. It was also found that stress ratio had an effect on the threshold stress intensity factors, with increasing stress ratio resulting in a smaller fatigue threshold value. Recommendations have been made for further experimentation with regard to threshold stress intensity factors of powdered aluminum alloys.

DETERMINATION OF THRESHOLD STRESS INTENSITY FACTORS FOR
7175-T651 ALUMINUM AND ALCOA MA-87 POWDERED ALUMINUM ALLOYS

I. INTRODUCTION

Background

Primary aircraft structural components generally contain flaws, defects, or anomalies of variable shape, orientation, and criticality, which are either inherent in the basic material or are introduced during the manufacturing and assembly processes. A large portion of service cracks found in aircraft structures are initiated from tool marks, manufacturing defects and the like (Ref 5).

In the past, the desire for more efficient aircraft structures has resulted in the selection and use of high strength alloys in primary members with little regard for the general decrease in fracture toughness associated with increased yield strength. The advantages of the higher yield strength, such as is available in certain steel, aluminum, and titanium alloys, are offset by a significant reduction in ductility, a factor that tends to enhance the possibility of failure by unstable fracture.

To date most experimental fatigue crack growth rate information has been obtained at growth rates of 10^{-7} inch/cycle and above which is suitable for a great many structural engineering applications. However, for structural components subjected to cyclic loading on the order of 10^{10} to 10^{12} cycles, investigation is warranted for the exploration of fatigue crack propagation growth rate behavior at or below 10^{-7} inch/cycle because of the many small loads at small stress intensities (Ref 4:126).

Literature Survey

Consideration of fatigue crack propagation is essential in the damage-tolerant approach to fatigue design. An empirical approach to crack propagation can be obtained by the application of fracture mechanics concepts to this subject. The most important aspect of the use of fracture mechanics is the single-valued correlation in the linear-elastic range between the stress intensity factor, K , and the rate of fatigue crack growth, da/dN , where " a " is the crack length and " N " is the number of cycles. K is the linear elastic fracture mechanics parameter that relates load, crack length, and structural geometry and is called the stress intensity factor because its magnitude determines the magnitude of the stress field in the crack tip region. Fatigue crack growth rate expressed as a function of crack-tip stress intensity range characterizes a materials resistance to stable crack extension under cyclic loading.

The characteristic dependence of rate of fatigue crack growth on the stress intensity factor is indicated in Figure 1. There are two asymptotic limits to the curve. The upper limit is set by the fracture toughness of the material, K_C . The lower limit is referred to as the threshold for crack growth, ΔK_{TH} . A practical threshold may be described as that ΔK below which fatigue crack growth rates become diminishingly small (Ref 11:142).

Many structural components have a higher probability for containing crack-like defects before going into service as in the case of welded joints. Some of these parts may have to be designed for durability throughout the service life time. In the absence of defects, this would

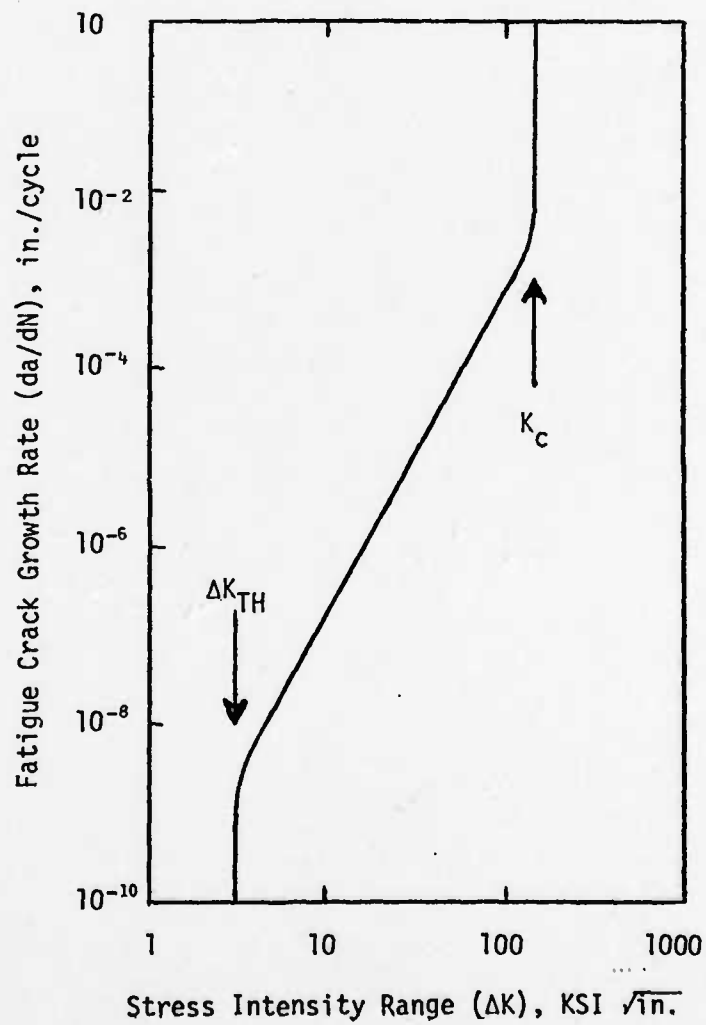


Figure 1. Schematic Illustration of the Fatigue Crack Growth Rate as a Function of Stress Intensity Range (Ref 6:10).

entail designing at stresses based on the 10^8 cycle life of the nominal stress versus elapsed cycles curve (S-N curve), but in the presence of defects the approach is to insure that the stress intensity associated with defects is kept below the threshold level for crack growth (Ref 9: 11).

In fracture mechanics large quantities of slow crack growth data under various combinations of cyclic and sustained loading are obtained and analyzed in terms of the crack tip stress intensity factor. An expression for the stress intensity factor for the single edge-cracked bend specimen (Ref 1) is

$$K = \frac{YM}{B(W - a)^{3/2}} \quad (1)$$

where

K = stress intensity factor

Y = dimensionless proportionality factor

M = moment

B = specimen thickness

W = specimen depth

and a = crack length

Equation (1) is based on results obtained from a boundary collocation analysis of the test specimen. The boundary collocation method was applied to the geometry and loading condition corresponding to a single edge-cracked specimen subjected to pure bending (4 point loading). The boundary collocation was carried out on the Williams stress function (Ref 14:109-114) and its normal derivative. In Figure 2 the points

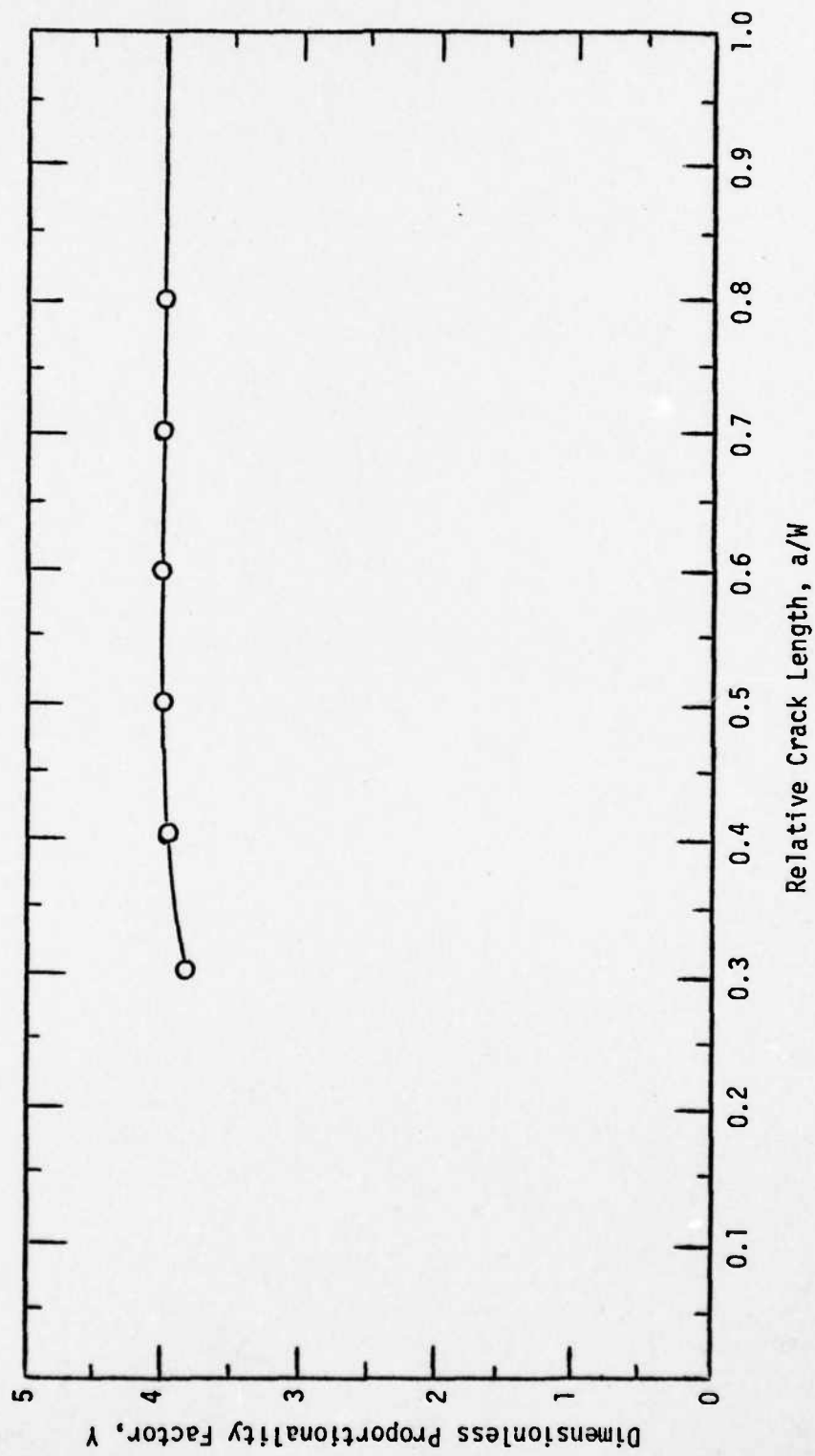


Figure 2. Dimensionless Proportionality Factors for Edge-Cracked Bend Specimen (Ref 15)

which represent stress intensities calculated for a number of specific crack lengths between $a/W = 0.3$ and 0.8 are shown. Each point represents a stable value over a wide range of collocation point numbers. The points shown are in excellent agreement with results previously presented (Ref. 3) over a smaller range of a/W .

In the limit the curve in Figure 2 must asymptotically approach a finite nonzero limit as a/W approaches 1.0 . A limiting value of 3.99 is reached for values of a/W greater than 0.6 . (Ref. 15:169-170).

Problem Definition

The purpose of this thesis was to obtain crack growth rate data and threshold stress intensity factors for two types of aluminum alloys: 7175-T651 aluminum and Alcoa MA-87 powdered aluminum. The scope of this study was limited to the experimental determination of threshold stress intensity factors utilizing a fatigue crack growth method for the edge-cracked bend specimen.

II. MATERIALS

Two types of aluminum alloys were used in this study: 7175-T651 wrought aluminum and a triple upset and rolled powdered aluminum alloy, Alcoa MA-87.

Chemical compositions of the two aluminum types are listed in Table I. Mechanical properties are listed in Table II. Heat treatment and aging processes are listed in Tables III and IV.

TABLE I

Chemical Composition (Weight Percent) of 7175-T651 and MA-87 Aluminum Alloys

Element	7175-T651*		MA-87**	
	Specification Limits	Materials Used	Specification Limits	Materials Used
Aluminum	Balance	Balance	Balance	Balance
Zinc	5.1 - 6.1	5.6	6.94 - 7.10	6.94
Magnesium	2.1 - 2.9	2.5	2.63 - 2.71	2.67
Copper	1.2 - 2.0	1.6	1.64 - 1.67	1.64
Chromium	0.18 - 0.30	0.25	0	0
Iron	0.20 max	0.20	0.6 max	0.6
Silicon	0.15 max	0.15	0.05 max	0.05
Manganese	0.30 max	0.10	0	0
Titanium	0.20 max	0.10	0	0
Cobalt	0	0	0.49 max	0.49
Others	0.15 max	0.15	0	0
*Ref. 2: **Ref. 7:				

TABLE II

Mechanical Properties of 7175-T651 and MA-87 Aluminum Alloys

Category	7175-T651*		MA-87**
	L-T Specimen	T-L Specimen	T-L Specimen
Yield Strength (0.2% Offset)	68.8 KSI	60.5 KSI	70.0 KSI
Ultimate Strength	87.5 KSI	85.1 KSI	80.0 KSI
Elongation	15.2%	13.1%	7.0%
*Ref. 2:16 **Ref. 7			

TABLE III

Heat Treatment and Aging Process of 7175-T651 Aluminum Alloy
(Ref. 2:23)

Semi-continuously cast 4 in. thick ingots		
Stress relieved overnight at 440°F		
Scalped to 3.375 in. thickness		
Held 1-2 hrs. at 860-870°F		
Homogenized for 15 hrs. at 920°F		
Cooled to 800-775°F		
Rolled to 1.75 in. thickness		
Reheated and rolled to 0.625 in. thickness		
Solution heat treated	0.5 hrs. at 880°F,	1.5 hrs. at 920°F
Quenched in ice water		
Stretched 1.5%		
Aged for 24 hrs. at 250°F		
Air cooled		

TABLE IV

Heat Treatment and Aging Process of MA-87 Aluminum Alloy
(Ref. 10:21)

Solution heat treated	2 hrs. at 910°F
Quenched in cold water	To room temperature
Naturally aged	5 days at room temperature
Artificially aged	24 hrs. at 250°F
Overaged	4 hrs. at 325°F
Air cooled	To room temperature

III. EXPERIMENTAL PROCEDURE

Threshold values of stress intensity factors were obtained for 7175-T651 and Alcoa MA-87 aluminum alloys using a crack growth procedure used by Johnson (Ref. 8). Cracks were periodically measured using Gaertner cathetometers in conjunction with auxillary lenses that were placed close to the specimen. Tests were conducted at minimum stress to maximum stress ratios (R ratios) of 0.1 and 0.3.

Test Apparatus

Tests were conducted on a Sonntag Universal fatigue testing machine. The function of the Sonntag testing machine was to apply a vertical vibratory force to a specimen mounting fixture attached between a heavy stationary frame and a reciprocating platen (Figure 3). The force to the specimen could have any static component from zero to 100 pounds, and any alternating component from zero to ± 100 pounds.

The vibratory force was produced by an unbalanced rotating mass supported between two bearings in a cage-like vertical frame, the top of which formed the reciprocating platen. The rotating mass was driven by a synchronous motor so that the speed was maintained constant at 1800 revolutions per minute (RPM).

The vertical component of the centrifugal force was the only component transmitted to the specimen. The horizontal component was absorbed by horizontal pivot rods which guided the reciprocating assembly in the vertical direction. Two horizontal tension springs kept the reciprocating assembly in position against the pivot rods (Ref. 12:1).

THIS PAGE IS BEST QUALITY PRACTICABLE
FROM COPY FURNISHED TO DDG

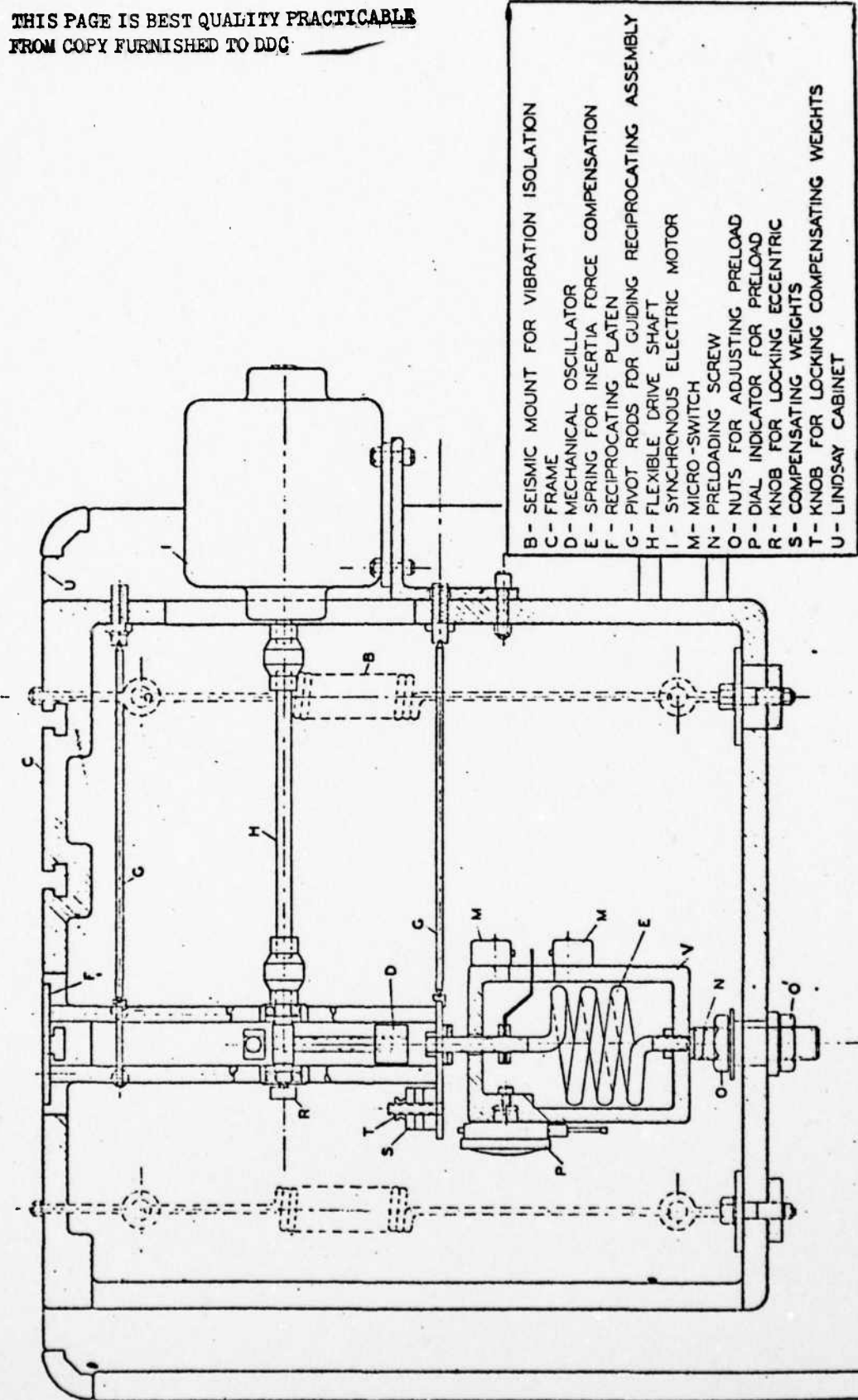


Figure 3. Schematic of Sonntag Universal Fatigue Testing Machine

Specimen Configuration

Edge-cracked bend specimens (Figure 4) were used for all tests. The length of each specimen was nominally five inches. Depth and thickness were nominally 0.4 inch. The initial notch depth was nominally 0.1 inch.

Specimen Preparation

All but one of the 7175 specimens were machined so that the crack growth would be perpendicular to the rolling direction (i.e. L-T, longitudinal-transverse) (Figure 5). One 7175 specimen was machined so that the crack growth would be parallel to the rolling direction (i.e. T-L, transverse-longitudinal) (Figure 6). All MA-87 specimens were machined in the T-L direction.

Each specimen was polished in the following manner to make the crack tip more visible: 320 grit paper was used first, then the angle of the specimen was changed 90 degrees and 400 grit paper was used, the angle was changed 90 degrees again and 500 grit paper was used, then 15 micron diamond paste was used in a circular motion, and finally six micron diamond past was used in a circular motion.

Testing

Continuous data on load, number of cycles, and crack length was maintained throughout testing. Static and alternating loads were reduced at various intervals based on plots of average crack length versus ΔP , where $\Delta P = P_{\max} - P_{\min}$, and average crack length versus number of cycles. P_{\max} was the maximum load and P_{\min} was the minimum load to the specimen produced by a combination of the alternating load (created by a rotating mass) and the static load. A step shedding of load was employed with the

All measurements in inches

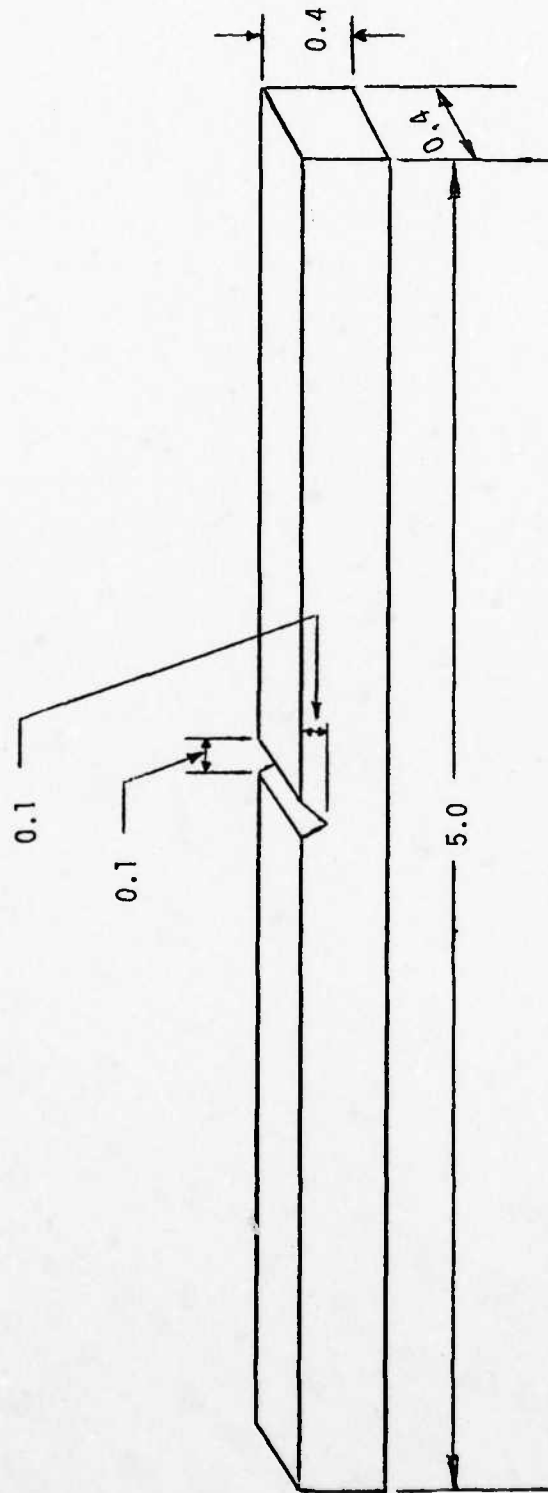


Figure 4. Edge-Cracked Bend Specimen

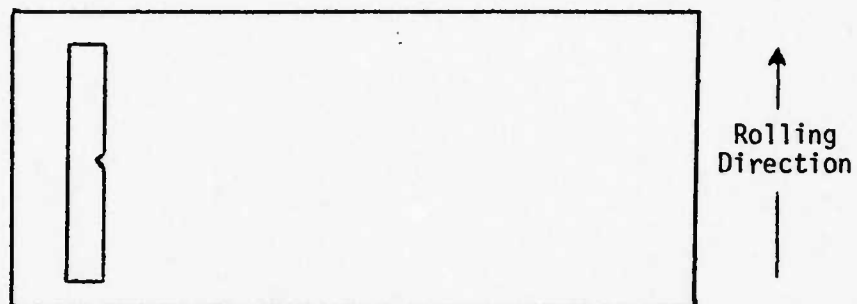


Figure 5. L-T (Longitudinal-Transverse) Specimen

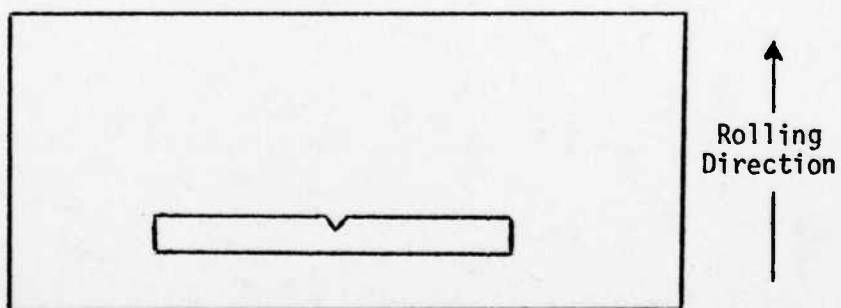


Figure 6. T-L (Transverse-Longitudinal) Specimen

reduction in ΔP to the adjacent load step not exceeding 20 percent for the first two steps, thereafter, a reduction rate of 10 percent was used (Figure 7). The step shedding method was used to asymptotically approach the threshold stress intensity by reducing the load to the specimen, thereby reducing stress intensity as the crack became longer.

Crack Measurement

Crack lengths on both sides of the specimen were periodically measured to determine crack growth rate. Crack lengths were determined visually by use of Gaertner cathetometers and auxillary lenses that were placed close to the specimen (Figure 8 and 9). All measurements were made with a static load on the specimen which enabled the crack to remain open and the crack tip to be clearly defined. A parallex in the Gaertner cathetometer could have produced errors of plus or minus 0.002 inch in the crack length, however, care was taken to ensure that all crack measurements were taken with the eye at the same level. Mylar tape with 0.005 inch divisions was attached to both sides of the specimen as reference marks for crack measurement. A high intensity lamp was used to highlight the crack tip. The combination of the cathetometer, auxillary lens, mylar tape, and constant eye position enabled accurate crack tip measurement to within plus or minus 0.002 inch.

Laboratory environmental conditions were room temperature (60° to 86°F over the test period) and relative humidity greater than 40 percent and less than 70 percent, both of which were recorded at intervals during testing. Relative humidity was determined by the use of a wet-and-dry bulb sling psychrometer.

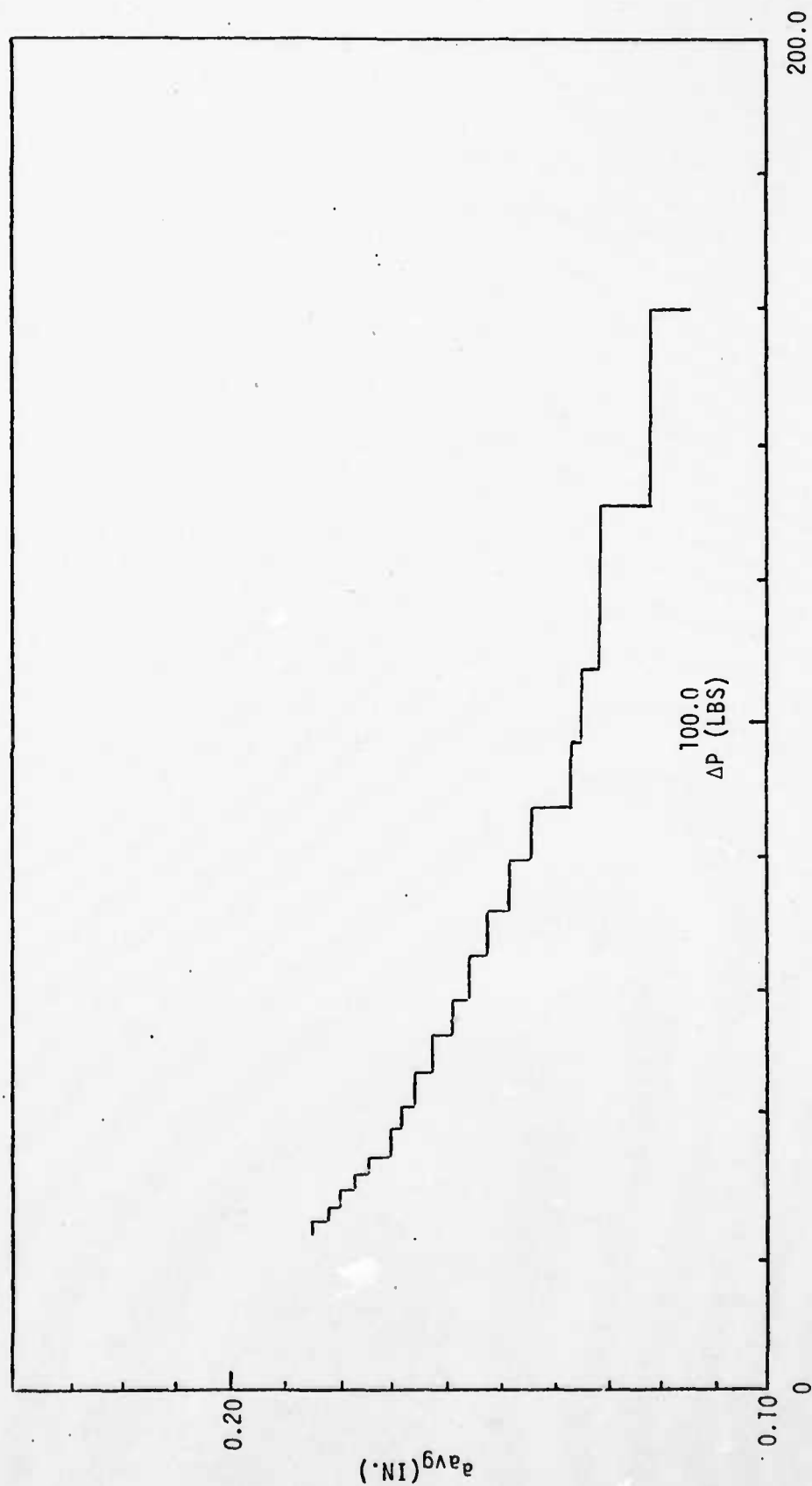


Figure 7. Average Crack Length Versus $\Delta P (\Delta P = P_{max} - P_{min})$ for Specimen #7(7175-T651 L-T, R = 0.1)

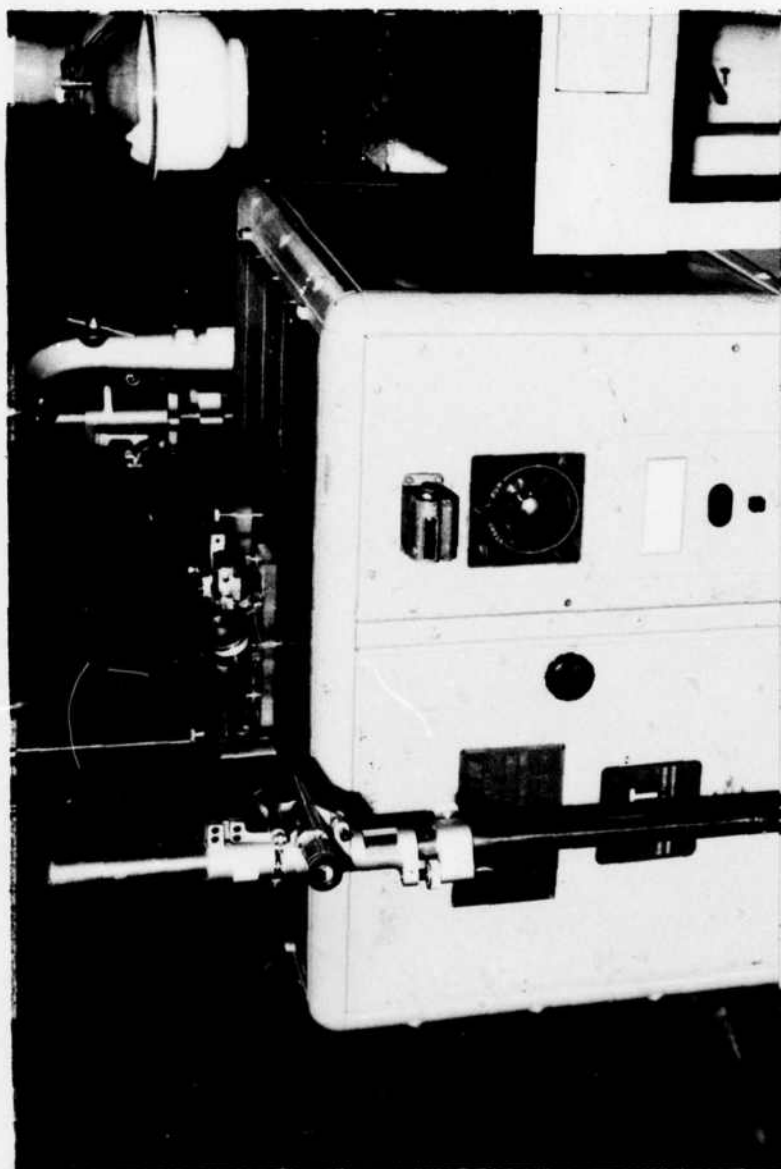


Figure 8. Sonntag Universal Fatigue Testing Machine

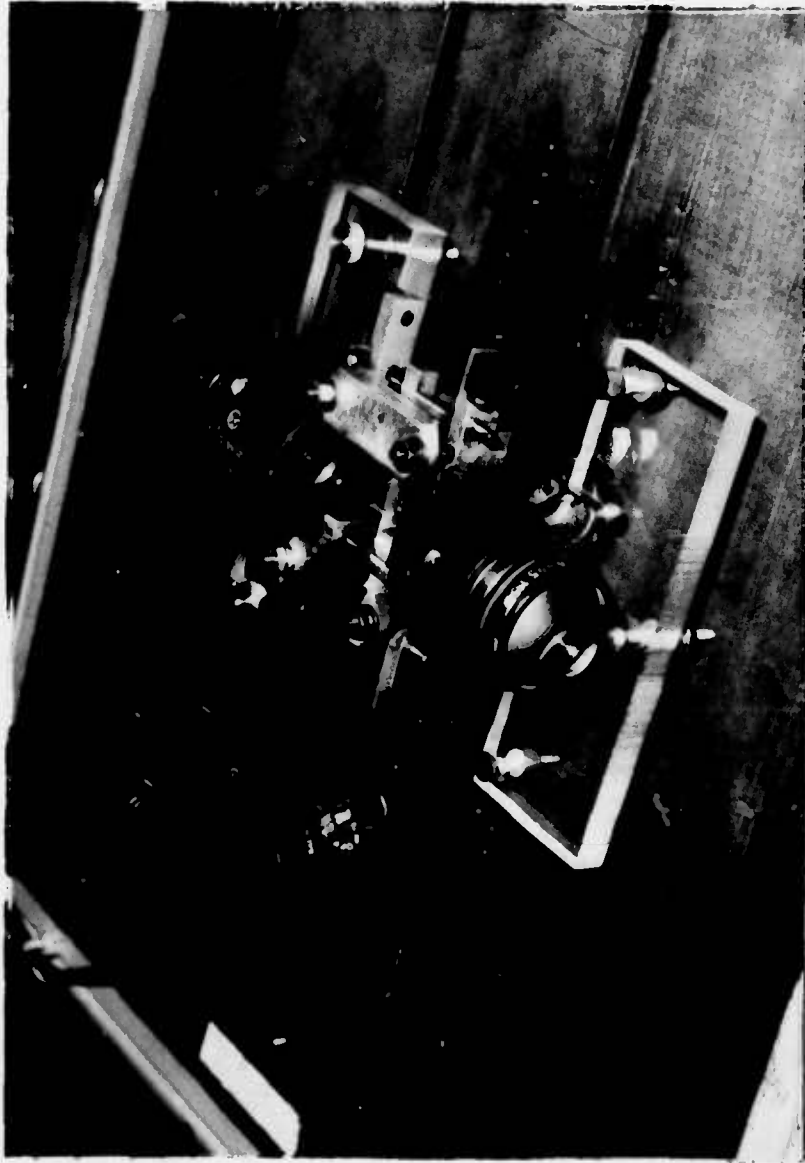


Figure 9. Edge-Cracked Bend Specimen Mounted in Sonntag Universal Fatigue Testing Machine

Post-test Measurement

Upon crack arrest and test completion (no change in crack length for 10 million cycles) the specimens were broken in half and the crack front was photographed (e.g. Figures 10 and 11). Five measurements were taken across the crack front at one-quarter intervals, including the two end points, in order to account for crack front curvature in the calculation of ΔK . This curvature was assumed to be constant for plotting crack growth rate, $\Delta a/\Delta N$, versus stress intensity factor range, ΔK . Table V shows the comparison of visual measurements taken during the tests and post-test measurements taken from photographs of the crack front.

Data Reduction

The rate of fatigue crack growth was determined from the average crack length versus elapsed cycles (a_{avg} vs. N) data by means of the secant method. The secant method or point-to-point technique involved calculating the slope of the straight line connecting two adjacent data points on the a_{avg} vs. N curve. In equation form the secant method can be expressed as

$$\frac{da}{dN} = \frac{a_{i+1} - a_i}{N_{i+1} - N_i} \quad (\text{Ref. 13:A1}) \quad (2)$$

Stress intensity factors at various moments and crack lengths were determined using the formula

$$\Delta K = \frac{Y \Delta M}{B(W - a)^{3/2}} \quad (3)$$

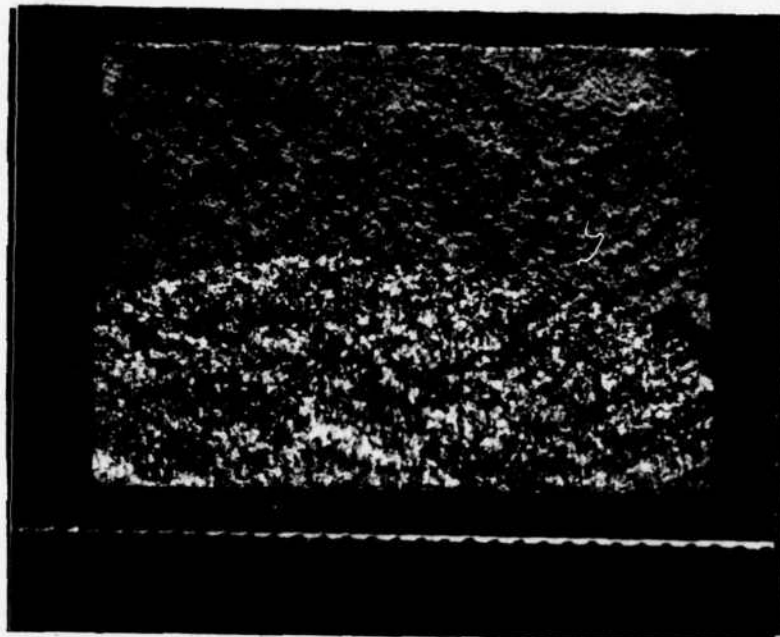


Figure 10. 7175-T651 Fracture Surface
(Divisions in 1/64 inch)

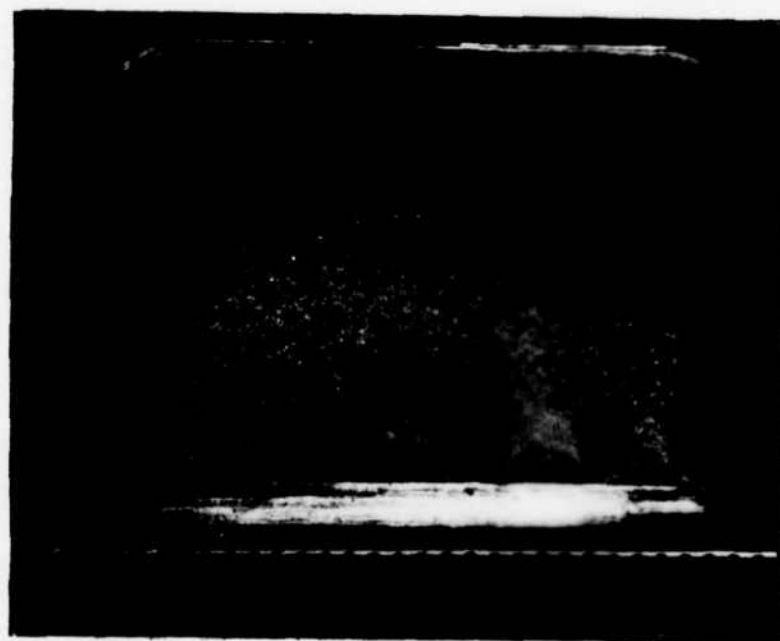


Figure 11. Alcoa MA-87 Fracture Surface
(Divisions in 1/64 inch)

TABLE V
Comparison of Visual and Post-Test Crack Measurements

Specimen	Measurement (inches)			
	Visual	Photograph	Visual	Photograph
# 1	0.097	0.101	0.110	0.111
# 6	0.114	0.118	0.049	0.047
# 7	0.063	0.069	0.077	0.078
# 8	0.066	0.068	0.087	0.086
# 9	0.096	0.099	0.127	0.127
#10	0.074	0.081	0.108	0.111
#13	0.064	0.063	0.041	0.039
#15	0.126	0.129	0.121	0.121
#16	0.139	0.139	0.091	0.097

IV. RESULTS AND DISCUSSION

Threshold stress intensity factors were determined experimentally for edge-cracked bend specimens by the crack growth method on the Sonntag Universal testing machine. Tests were conducted at stress ratios ($R = P_{\min}/P_{\max}$) of $R = 0.1$ and $R = 0.3$. Crack lengths were measured visually on both sides of the specimen using Gaertner cathetometers coupled with auxillary lenses placed close to the specimen.

Static and cyclic loads were reduced at various intervals (with R held constant) based on plots of average crack length, a_{avg} , versus ΔP , where $\Delta P = P_{\max} - P_{\min}$ (Figure 7), and average crack length versus number of cycles (Figure 12). Upon crack arrest and test completion (no change in crack length for 10 million cycles), specimens were broken in half and the crack front was photographed. Five measurements were taken across the crack front at one-quarter intervals, including the two end points to calculate ΔK , to develop the plot of crack growth rate, $\Delta a/\Delta N$, versus stress intensity factor range, ΔK (Figure 13).

Table VI compares the results of the nine completed tests. A comparison of the two aluminum alloys shows that 7175-T651 had a greater fatigue threshold at the same stress ratio than the powdered MA-87. Table VI also shows the one 7175-T651 transverse-longitudinal specimen which was tested had a slightly lower fatigue threshold value than did the three 7175-T651 longitudinal-transverse specimens.

A plot of threshold stress intensity values versus stress ratio (ΔK_{TH} vs. R) shows that stress ratio had an effect on the threshold values of ΔK with increasing stress ratio resulting in a smaller fatigue threshold (Figure 14).

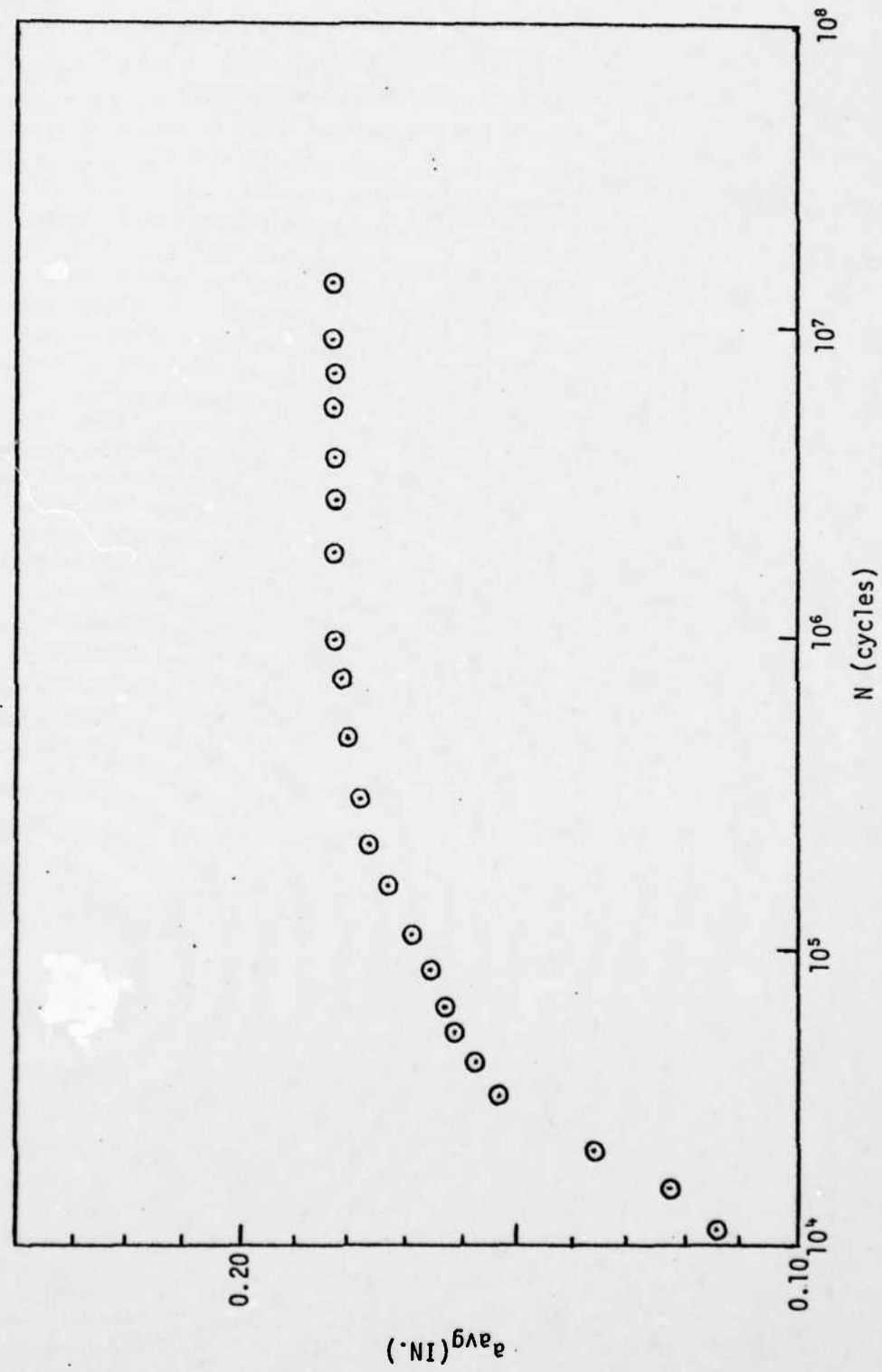


Figure 12. Average Crack Length Versus Number of Cycles for Specimen #7 (7175-T651 L-T, $R = 0.1$)

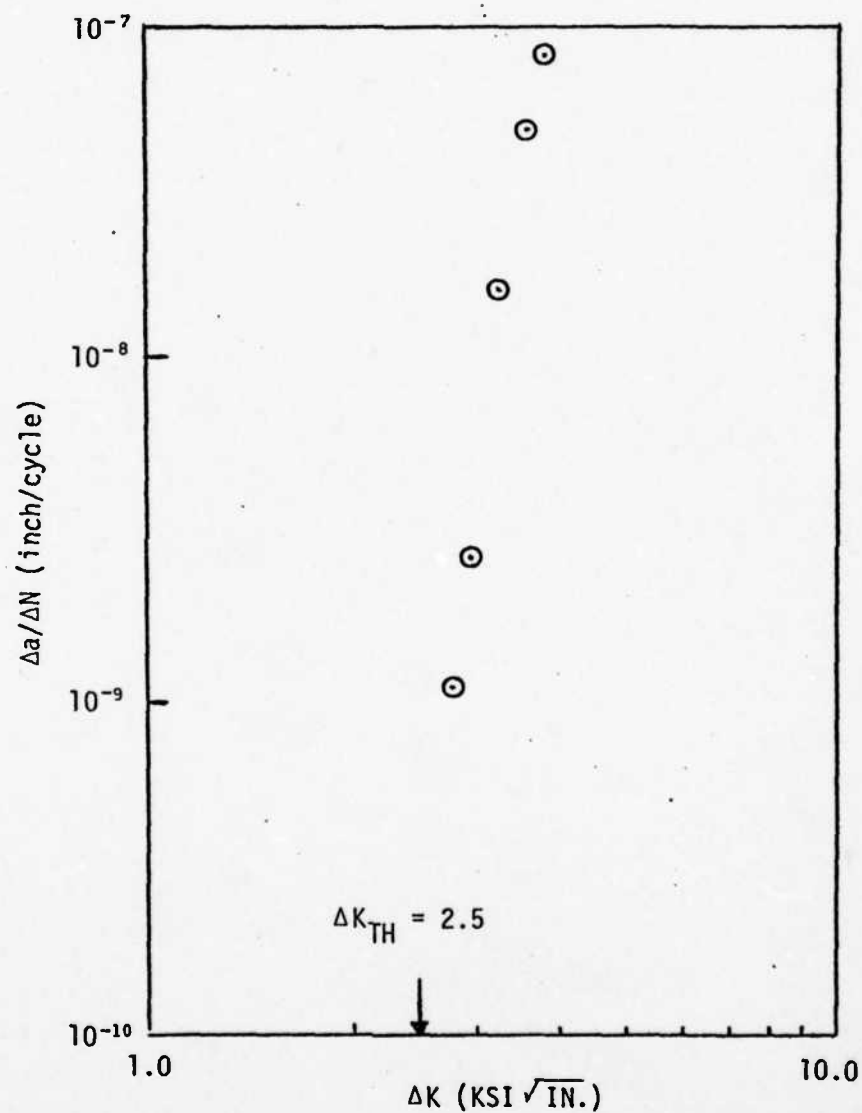


Figure 13. Fatigue Crack Growth Rate Versus Stress Intensity Factor Range for Specimen #7 (7175-T651 L-T, R = 0.1)

TABLE VI

Threshold Stress Intensity Factor Tests (ΔK_{TH} in KSI $\sqrt{\text{IN.}}$)

Aluminum Alloy	ΔK_{TH} at R = 0.1	ΔK_{TH} at R = 0.3
7175-T651 L-T	2.4	2.2
	2.5	1.8
	2.3	
7175-T651 T-L	2.1	-
MA-87 T-L	1.6	0.9
	1.1	

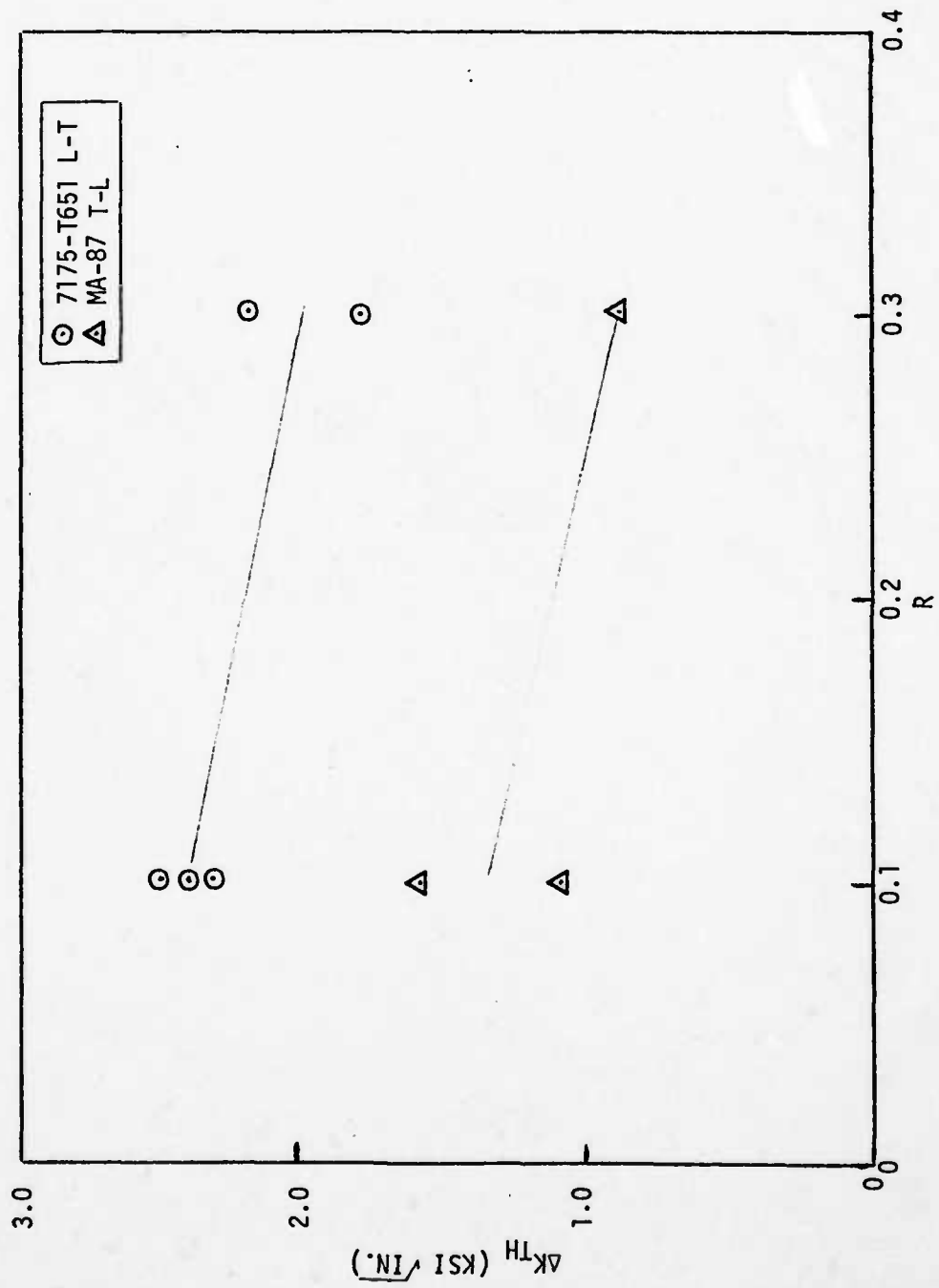


Figure 14. Threshold Stress Intensity Factors Versus Stress Ratio

V. CONCLUSIONS AND RECOMMENDATIONS

Conclusions

An experimental study to determine the threshold stress intensity factors for two aluminum alloys: 7175-T651 and a new powdered alloy, Alcoa MA-87, resulted in the following conclusions.

1. A comparison of the two aluminum alloys showed 7175-T651 to have a greater fatigue threshold, ΔK_{TH} , at the same stress ratio, R , than Alcoa MA-87.
2. Stress ratio was found to have an effect on the fatigue threshold with increasing R resulting in a smaller ΔK_{TH} value.
3. The crack growth test method employed by Johnson was found to be a suitable means for obtaining threshold stress intensity factors for the two aluminum alloys. Visual measurements of the arrested crack tip taken during tests agreed well with measurements taken from photographs of the crack front after the specimen was broken.

Recommendations

It is recommended that:

1. Further threshold tests be performed on powdered aluminum alloys at various stress ratios, R .
2. Further threshold tests be performed on powdered aluminum alloys fabricated from various forgings (i.e. triple upset and draw).

BIBLIOGRAPHY

1. ASTM Committee E-24, Proposed Method of Test for Plane-Strain Fracture Toughness on Metallic Materials. Book of ASTM Standards, Part 31, 1969.
2. Blau, P. J., Influence of Iron and Silicon Content on the Tensile Properties of 7x75 and ZR-Modified 7x75 Aluminum Plate - Technical Report AFML-TR-75-140, Wright-Patterson AFB, OH: Air Force Materials Laboratory, October 1975.
3. Brown, W. F., Jr., and J. E. Srawley. Plane Strain Crack Toughness Testing of High Strength Metallic Materials. ASTM STP 410, 1966.
4. Bulli, R. J., et al. "Fatigue Crack Propagation Growth Rates Under a Wide Variation of ΔK for ASTM A517 Grade F(T-1) Steel." Proceedings of the 1971 National Symposium on Fracture Mechanics, Part I, ASTM STP 513: Stress Analysis and Growth of Cracks. American Society for Testing and Materials: 177-195 (1972).
5. Donaldson, D. R. and W. F. Anderson. "Crack Propagation Behavior of Some Airframe Materials." Proceedings of the Crack Propagation Symposium, Vol. II. Cranfield: September 1974.
6. Gallagher, J. P. What the Designer Should Know About Fracture Mechanics Fundamentals. SAE 71015, New York: Society of Automotive Engineers, Inc., January 1971.
7. Griffith, W. M. Air Force Materials Laboratory - LLS, Wright-Patterson AFB, OH., Personal Communication, July 1977.
8. Johnson, R. E. Unpublished Research, 1977.
9. McEvelly, A. J. Fracture by Fatigue. Presented at the Mechanical Failures Prevention Group (MFPG Symposium on Mechanical Failures, Connecticut University, May 1974.
10. Otto, W. L., Jr. Metallurgical Factors Controlling Structure in High Strength P/M Products, AFML-TR-76-60, Alcoa Center, PA: Aluminum Company of America, Alcoa Technical Center, May 1976.
11. Paris, P. C., et al. "Extensive Study of Low Fatigue Crack Growth Rates in A533 and A508 Steels." Proceedings of the 1971 National Symposium on Fracture Mechanics, Part I, ASTM STP 513: Stress Analysis and Growth of Cracks. American Society for Testing and Materials: 141-176 (1972).
12. ---The Sonntag Universal Fatigue Machine, SF-01-U. Description of Machine. 90379-S, Sheet 1.
13. ---Tentative Method of Test for Constant Load Amplitude Fatigue Crack Growth Rates above 10^{-8} m/cycle. March 1977.

14. Williams, M. L. "On the Stress Distribution at the Base of a Stationary Crack." Journal of Applied Mechanics, 24, 109-114 (1957).
15. Wilson, W. K. "Stress Intensity Factors for Deep Cracks in the Bending and Compact Tension Specimens." Engineering Fracture Mechanics, Vol. 2, Great Britain: Pergamon Press, 1970.

APPENDIX A

Supplementary Data

APPENDIX A

Supplementary Data

Figures 15 through 38 are the individual crack growth tests. For each specimen average crack length, a_{avg} , is plotted versus ΔP , $\Delta P = P_{max} - P_{min}$, and number of cycles, N . Also crack growth rate, $\Delta a/\Delta N$, versus stress intensity factor range, ΔK , is plotted for each specimen.

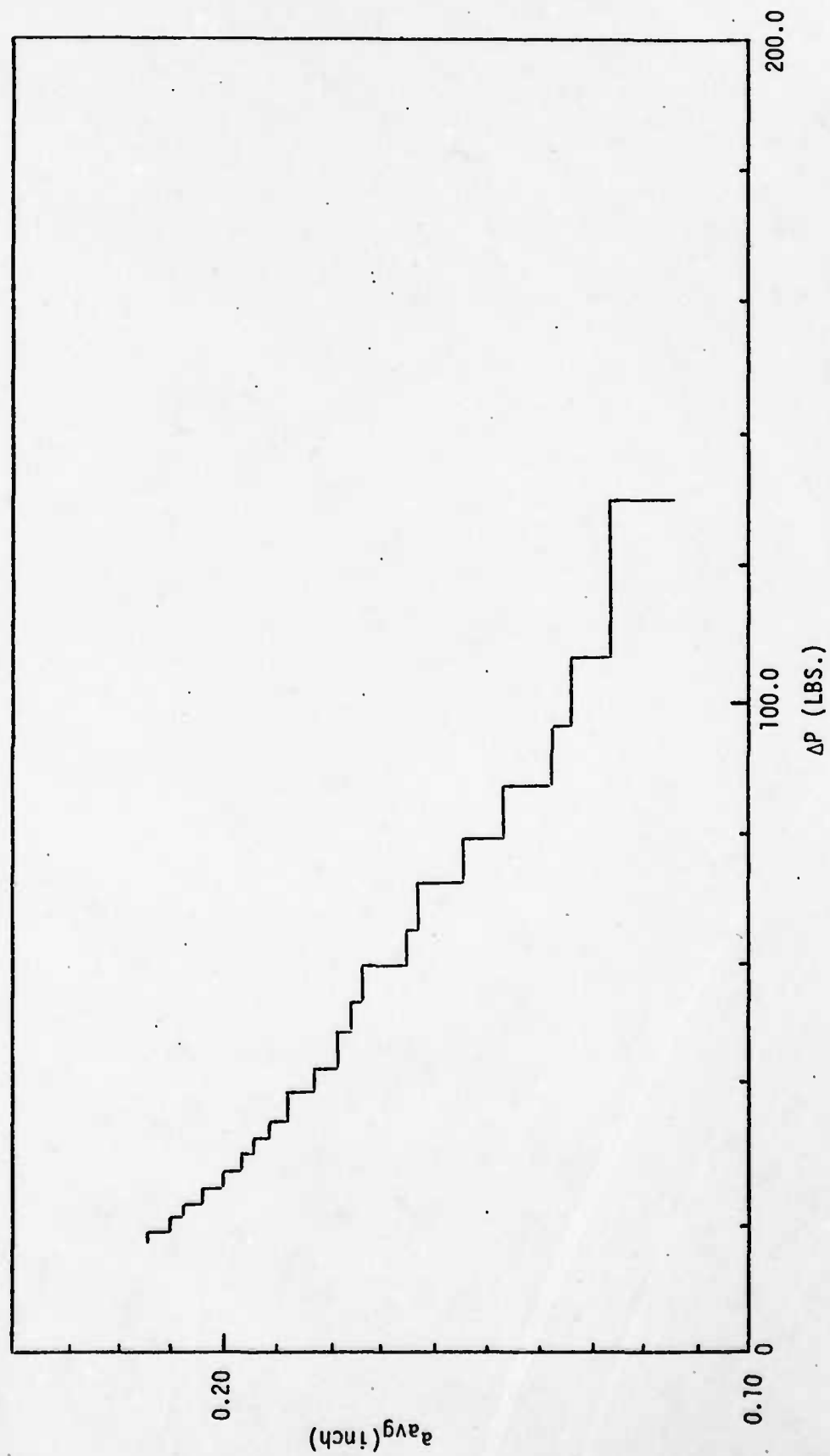


Figure 15. Average Crack Length Versus $\Delta P (\Delta P = P_{max} - P_{min})$ for Specimen #1 (7175-T651 T-L, $R = 0.1$)

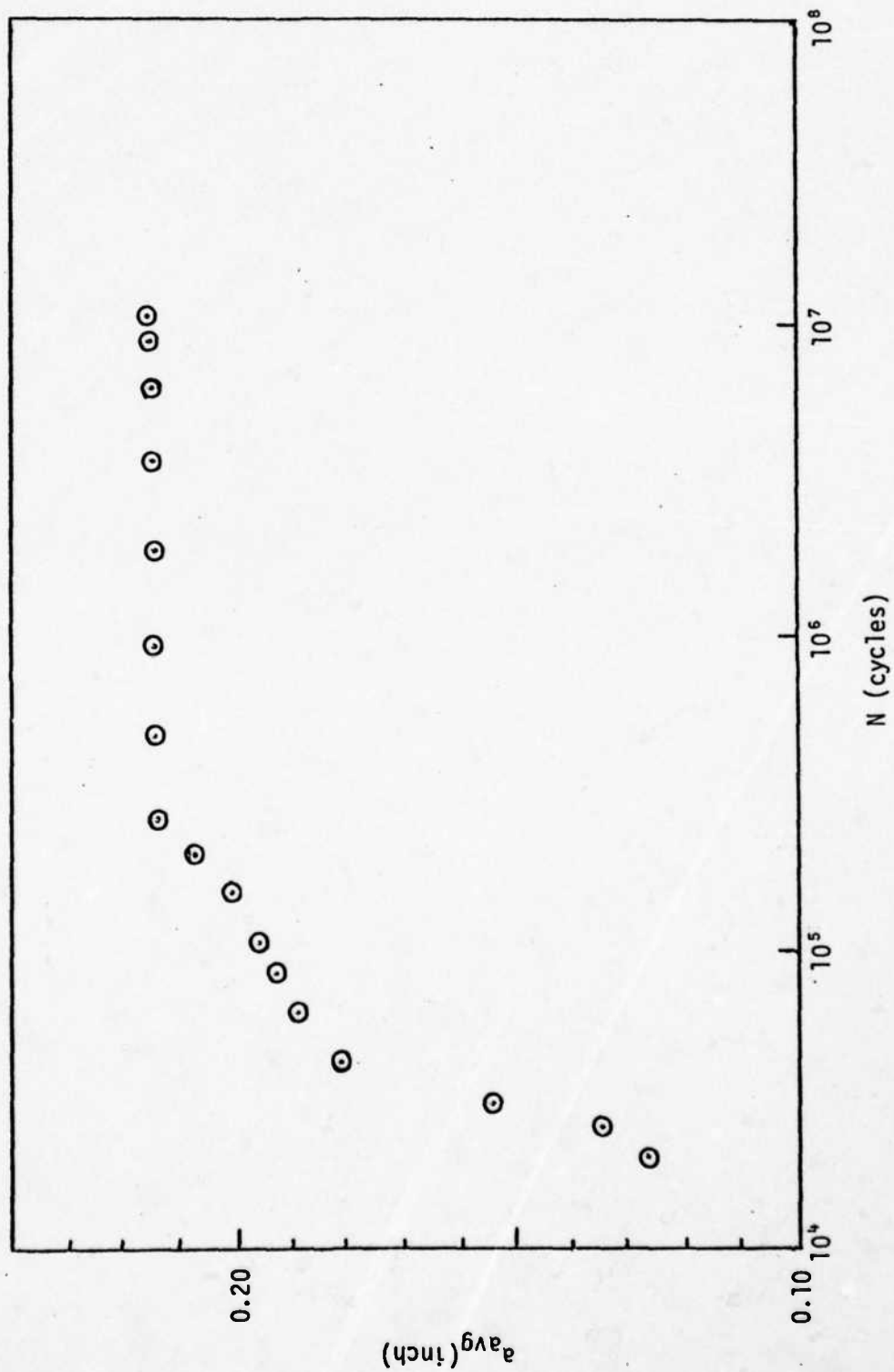


Figure 16. Average Crack Length Versus Number of Cycles for Specimen #1 (7175-T651 T-L, $R = 0.1$)

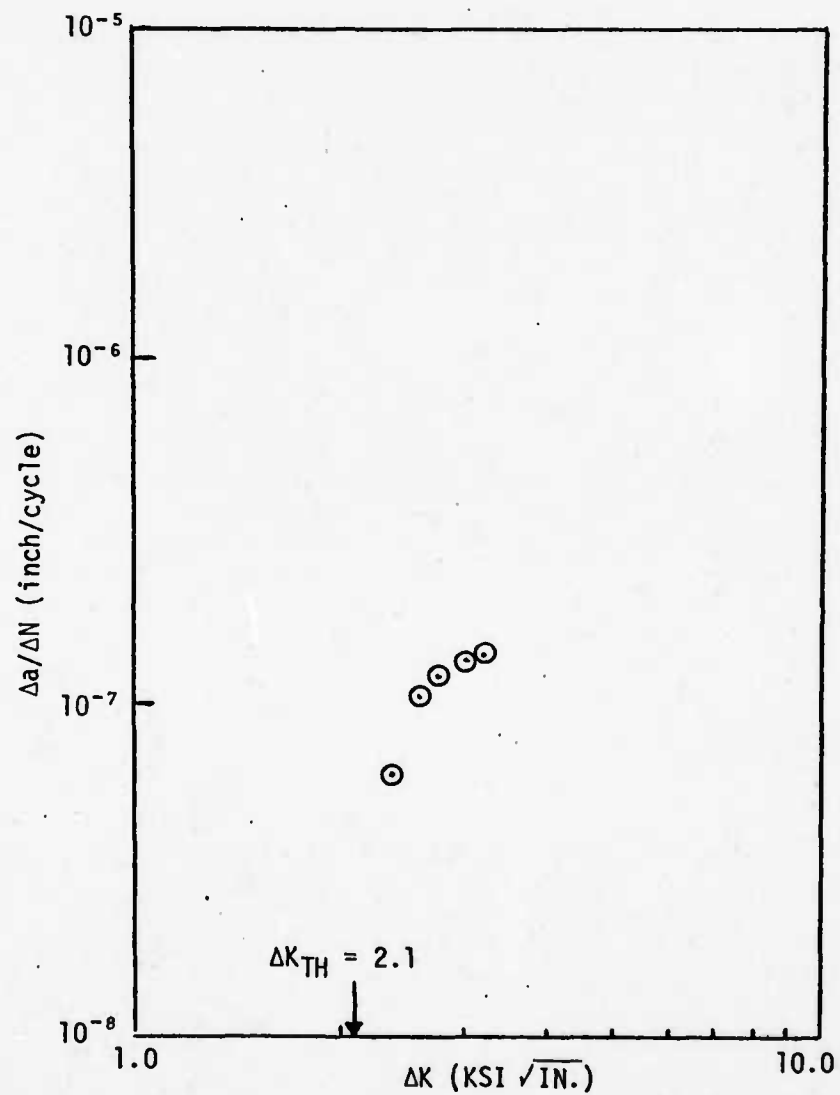


Figure 17. Fatigue Crack Growth Rate Versus Stress Intensity Factor Range for Specimen #1(7175-T651 T-L, R = 0.1)

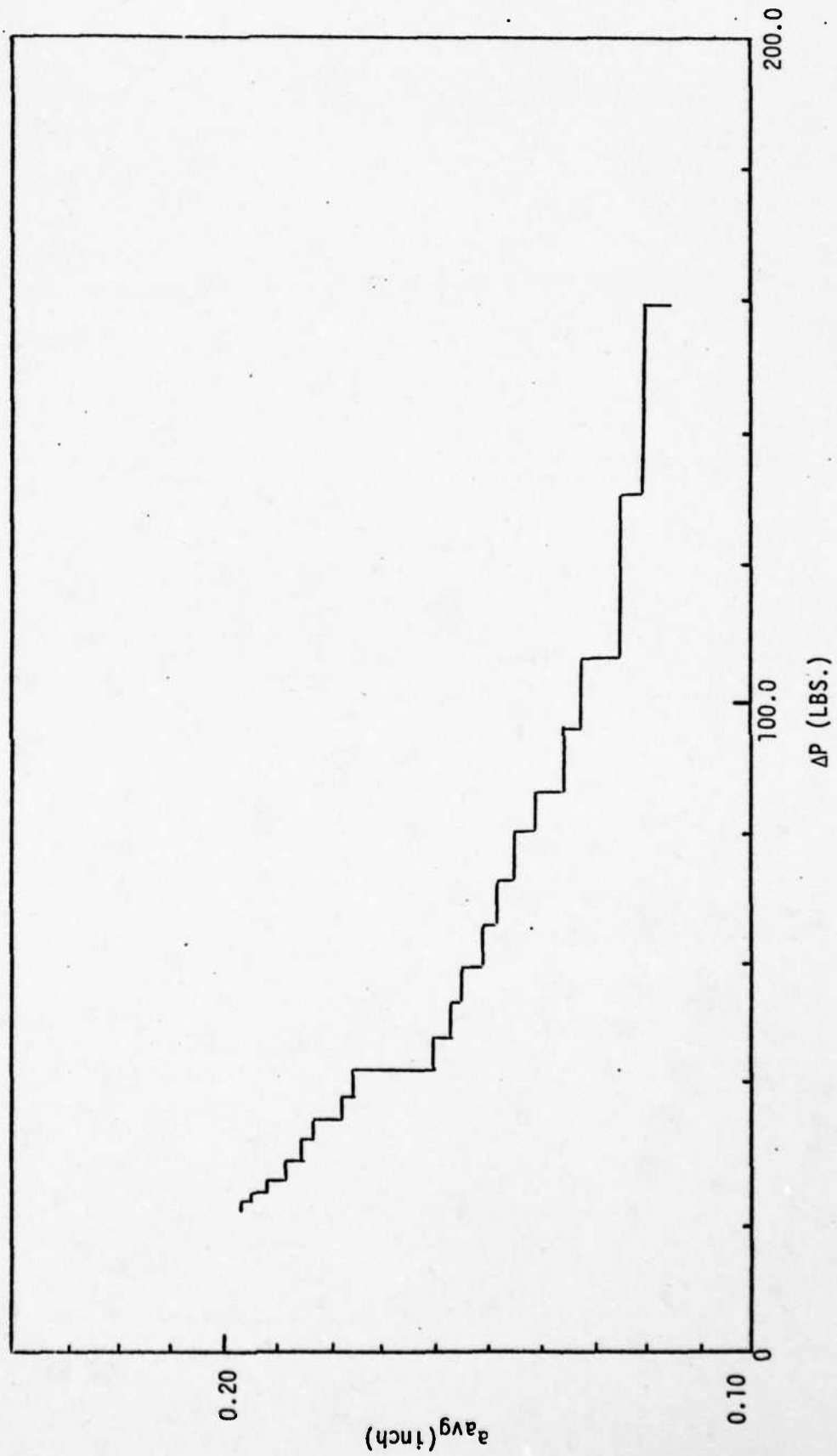


Figure 18. Average Crack Length Versus $\Delta P (\Delta P = P_{max} - P_{min})$ for Specimen #6(7175-T651 L-T, R = 0.1)

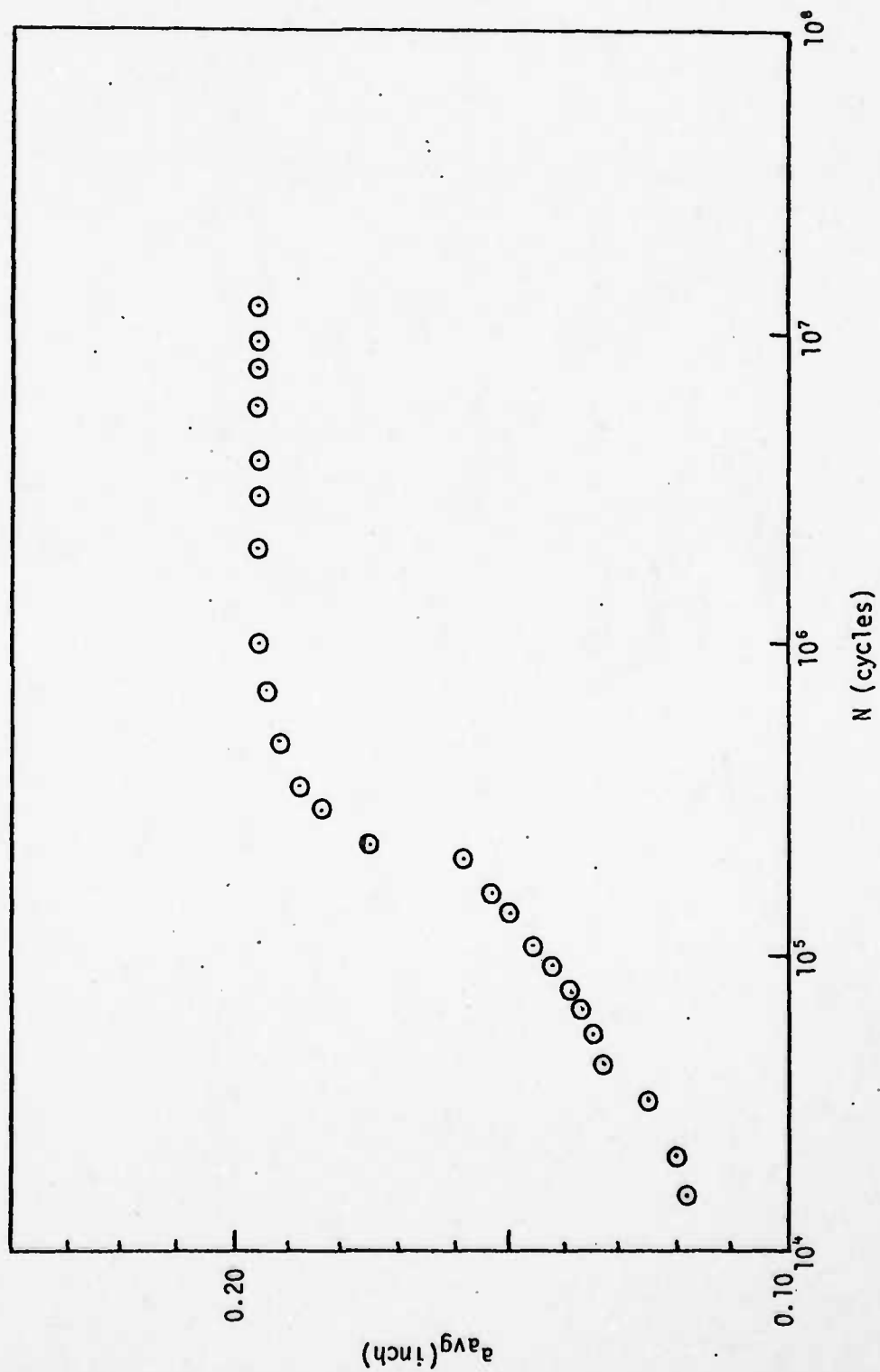


Figure 19. Average Crack Length Versus Number of Cycles for Specimen #6 (7175-T651 L-T, $R = 0.1$)

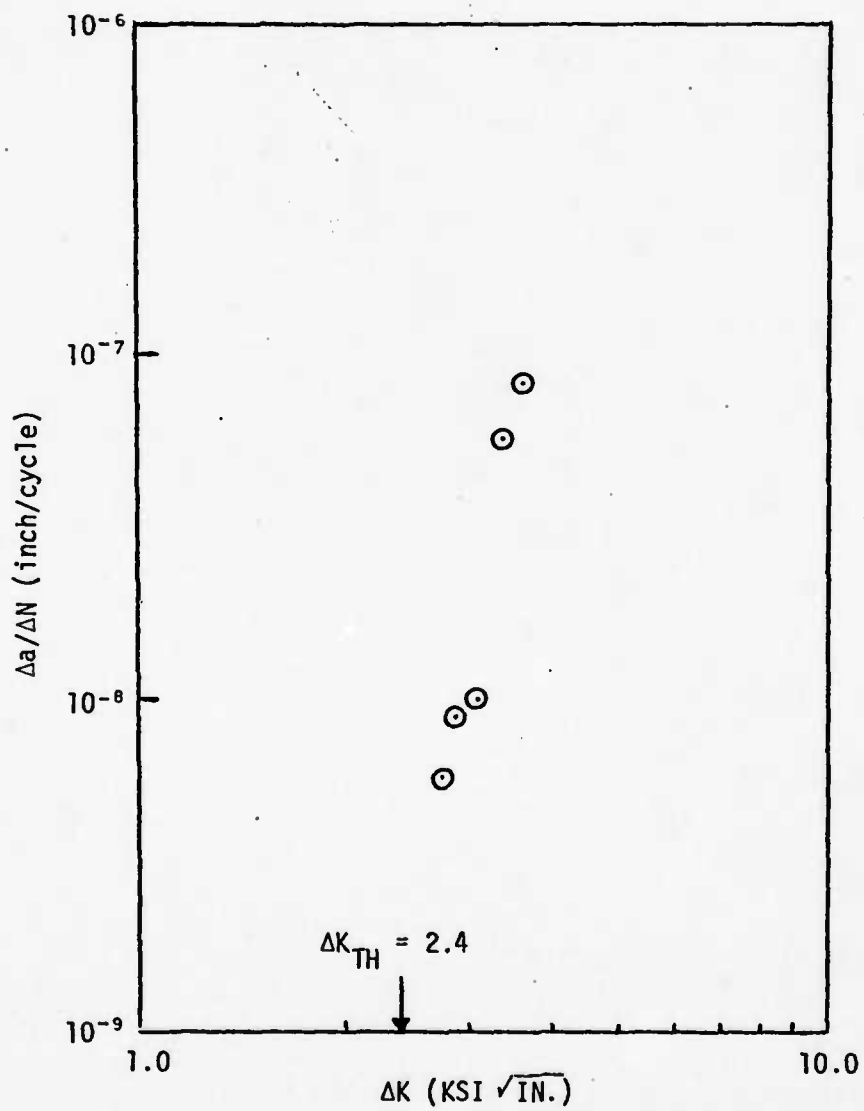


Figure 20. Fatigue Crack Growth Rate Versus Stress Intensity Factor Range for Specimen #6 (7175-T651 L-T, R = 0.1)

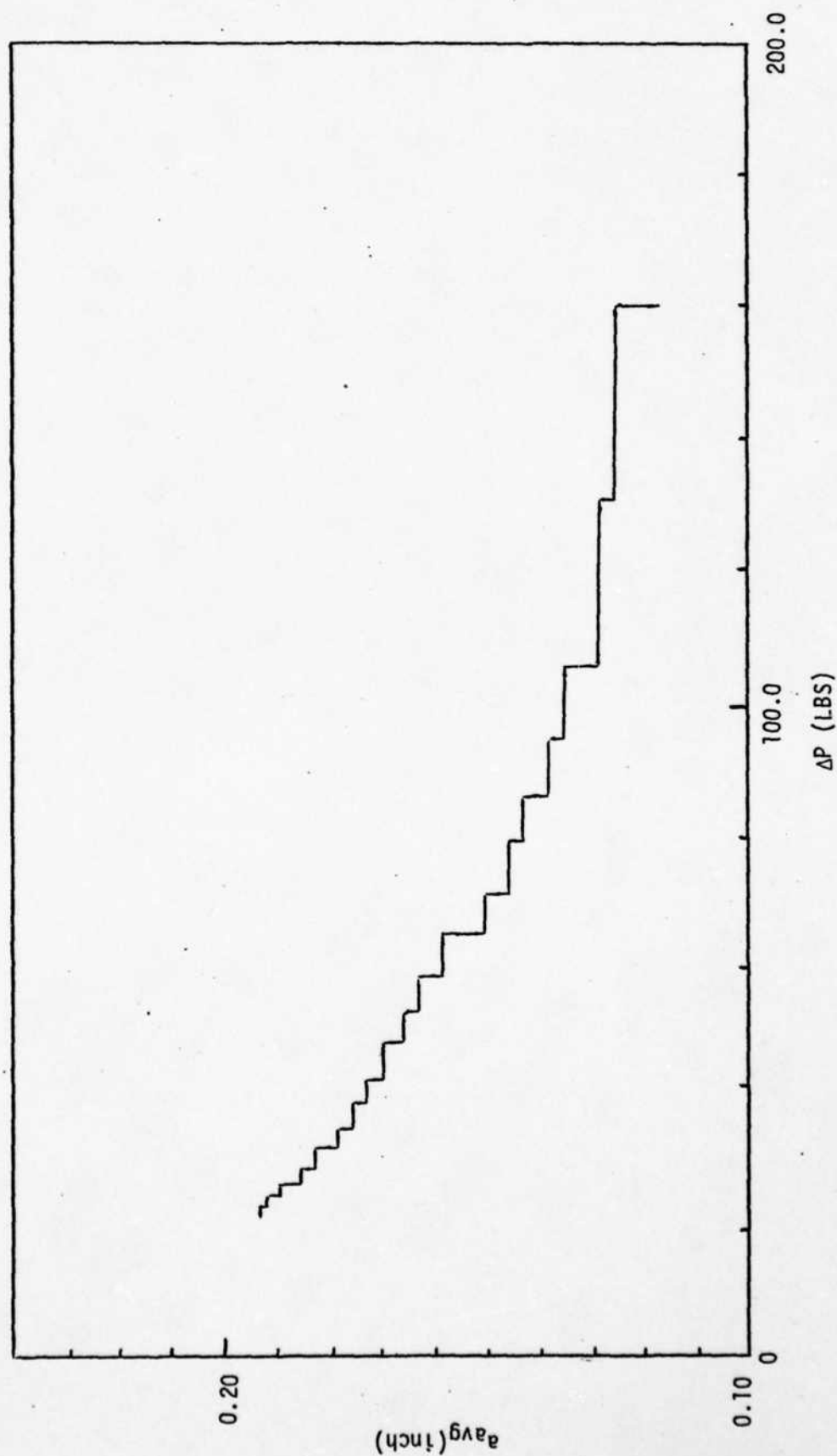


Figure 21. Average Crack Length Versus $\Delta P (\Delta P = P_{max} - P_{min})$ for Specimen #8 (7175-T651 L-T, $R = 0.1$)

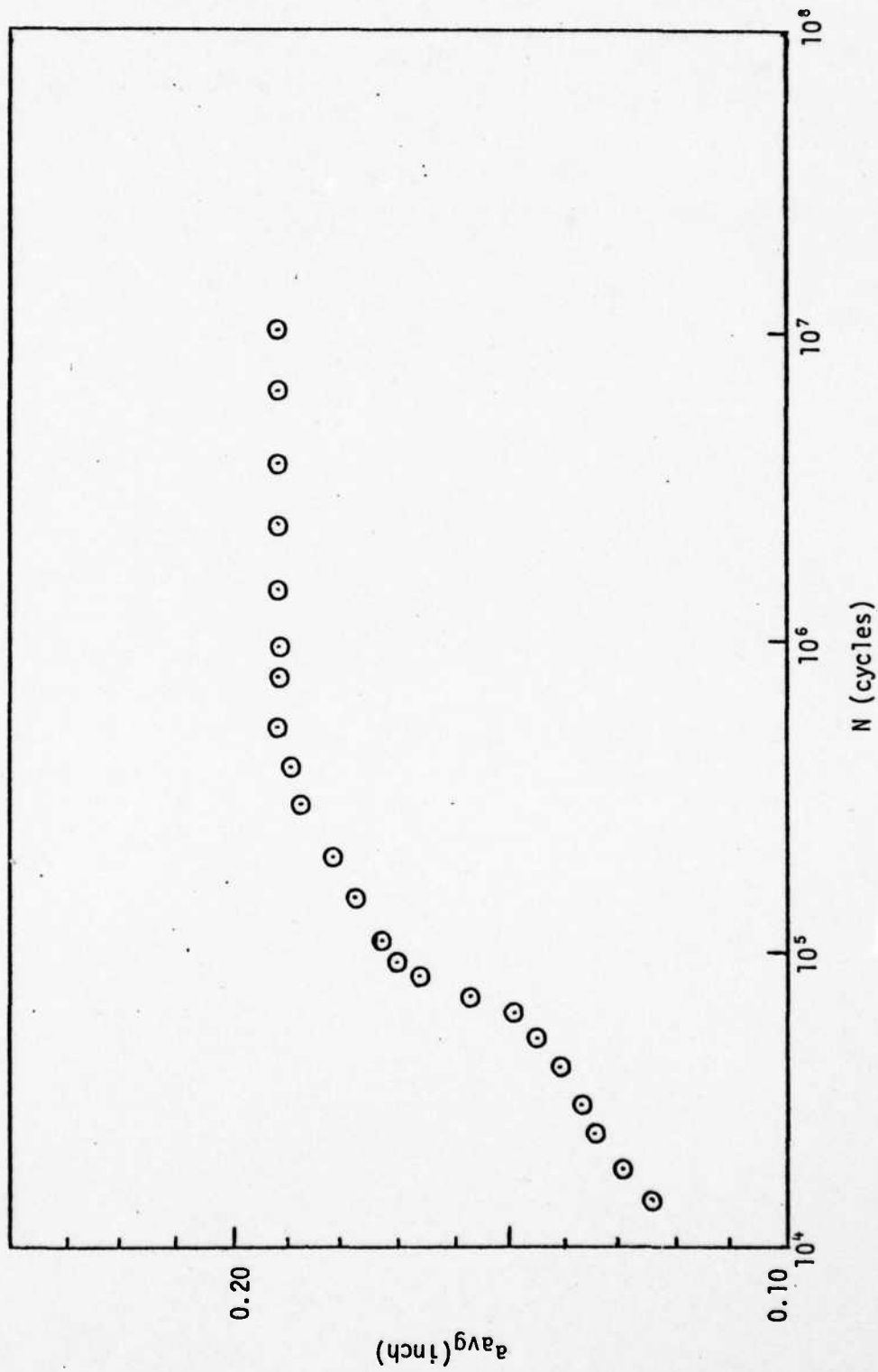


Figure 22. Average Crack Length Versus Number of Cycles for Specimen #8 (7175-T651 L-T, $R = 0.1$)

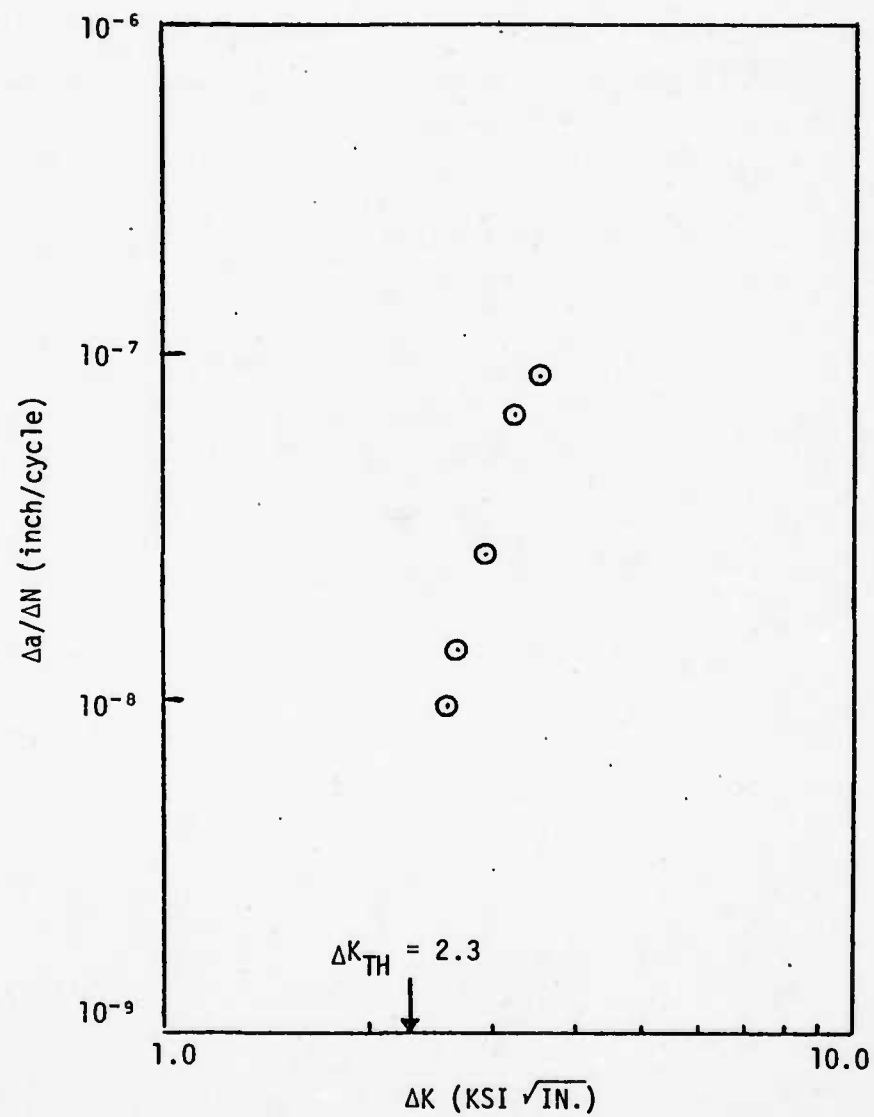


Figure 23. Fatigue Crack Growth Rate Versus Stress Intensity Factor Range for Specimen #8 (7175-T651 L-T, R = 0.1)

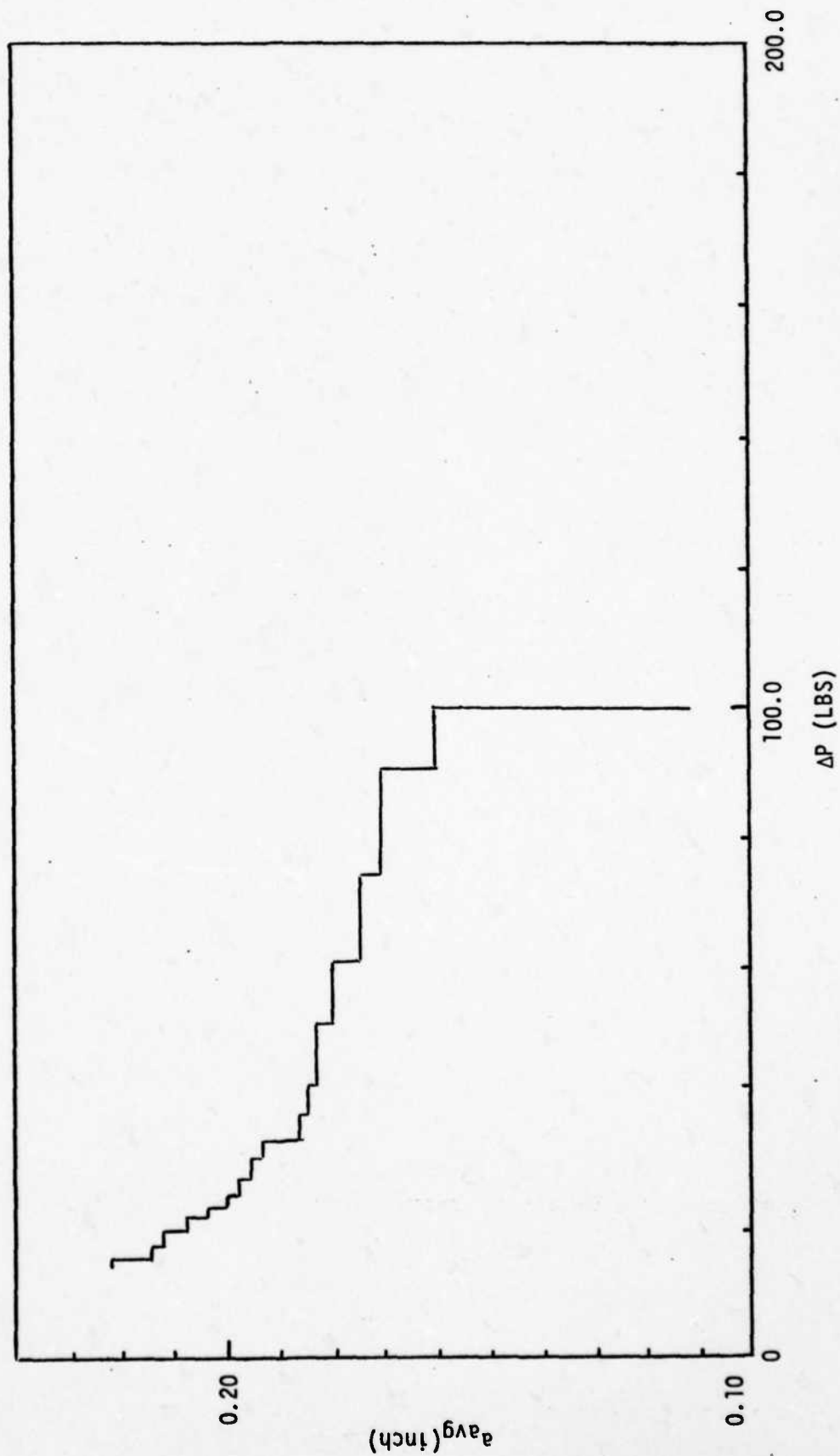


Figure 24. Average Crack Length Versus $\Delta P (\Delta P = P_{max} - P_{min})$ for Specimen #9 (7175-T651 L-T, $R = 0.3$)

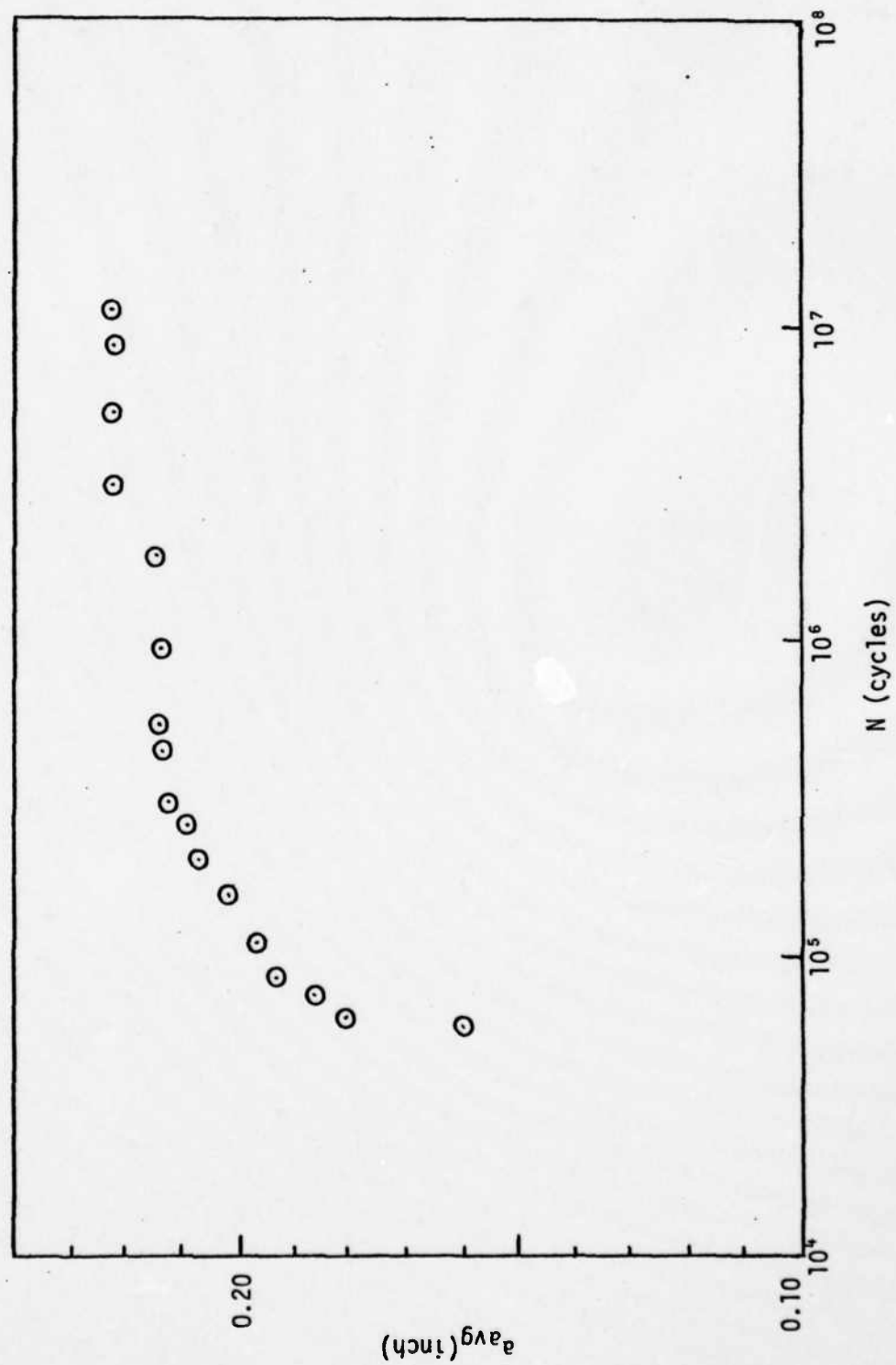


Figure 25. Average Crack Length Versus Number of Cycles for Specimen #9 (7175-T651 L-T, $R = 0.3$)

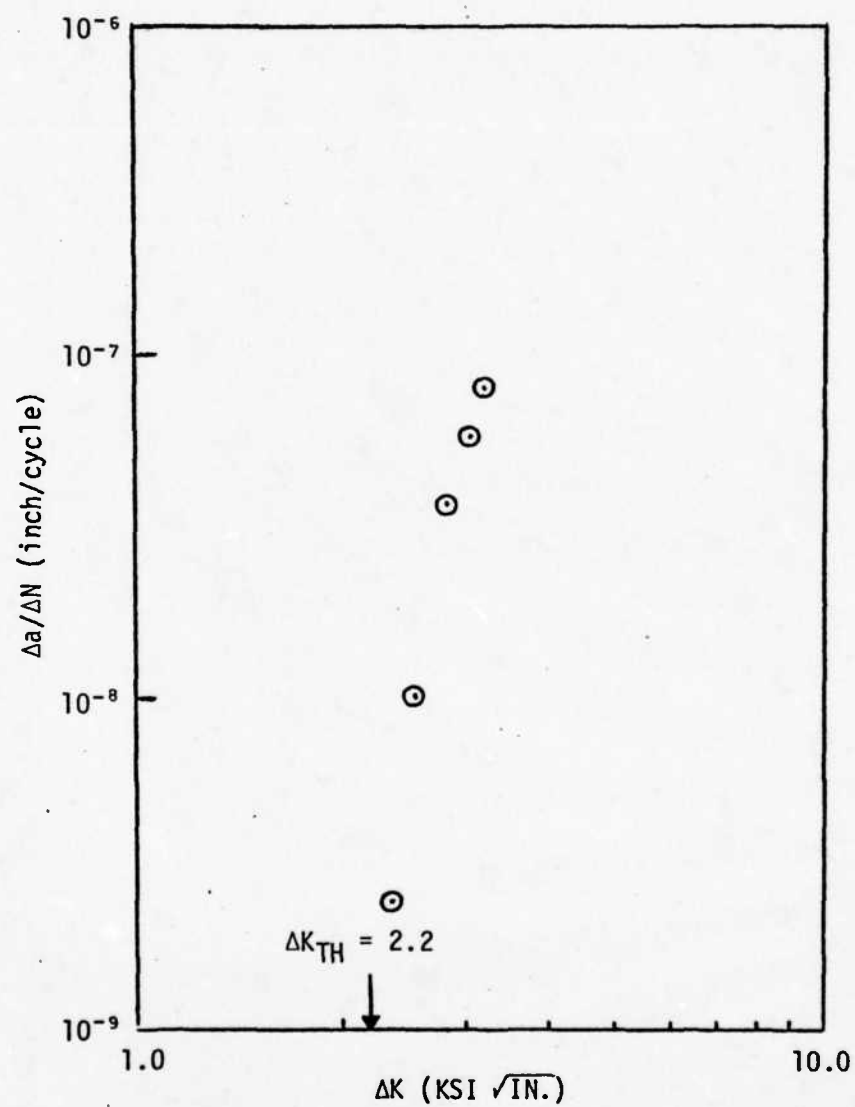


Figure 26. Fatigue Crack Growth Rate Versus Stress Intensity Factor Range for Specimen #9 (7175-T651 L-T, R = 0.3)

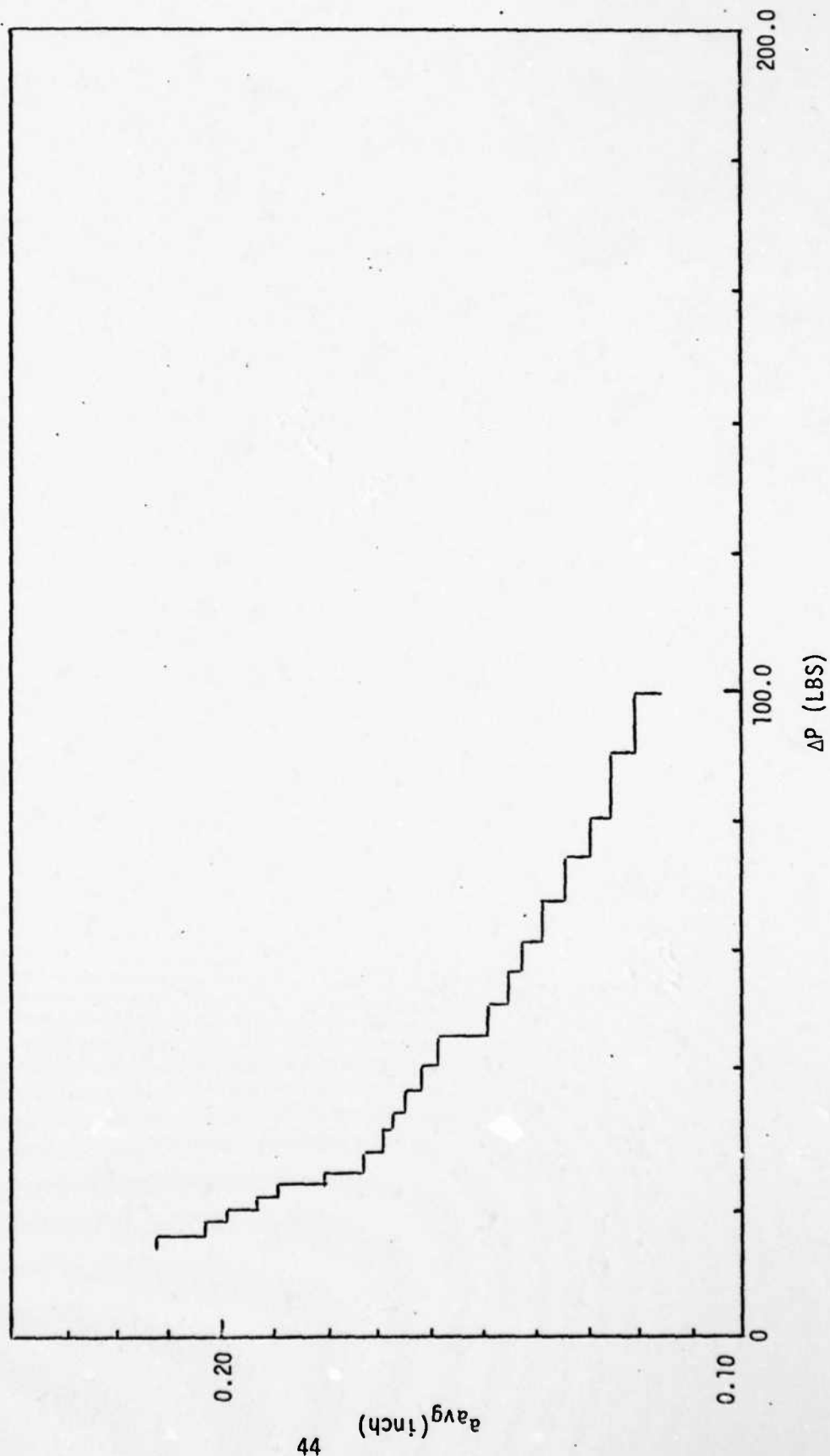


Figure 27. Average Crack Length Versus $\Delta P (\Delta P = P_{max} - P_{min})$ for Specimen #10 (7175-T651 L-T, $R = 0.3$)

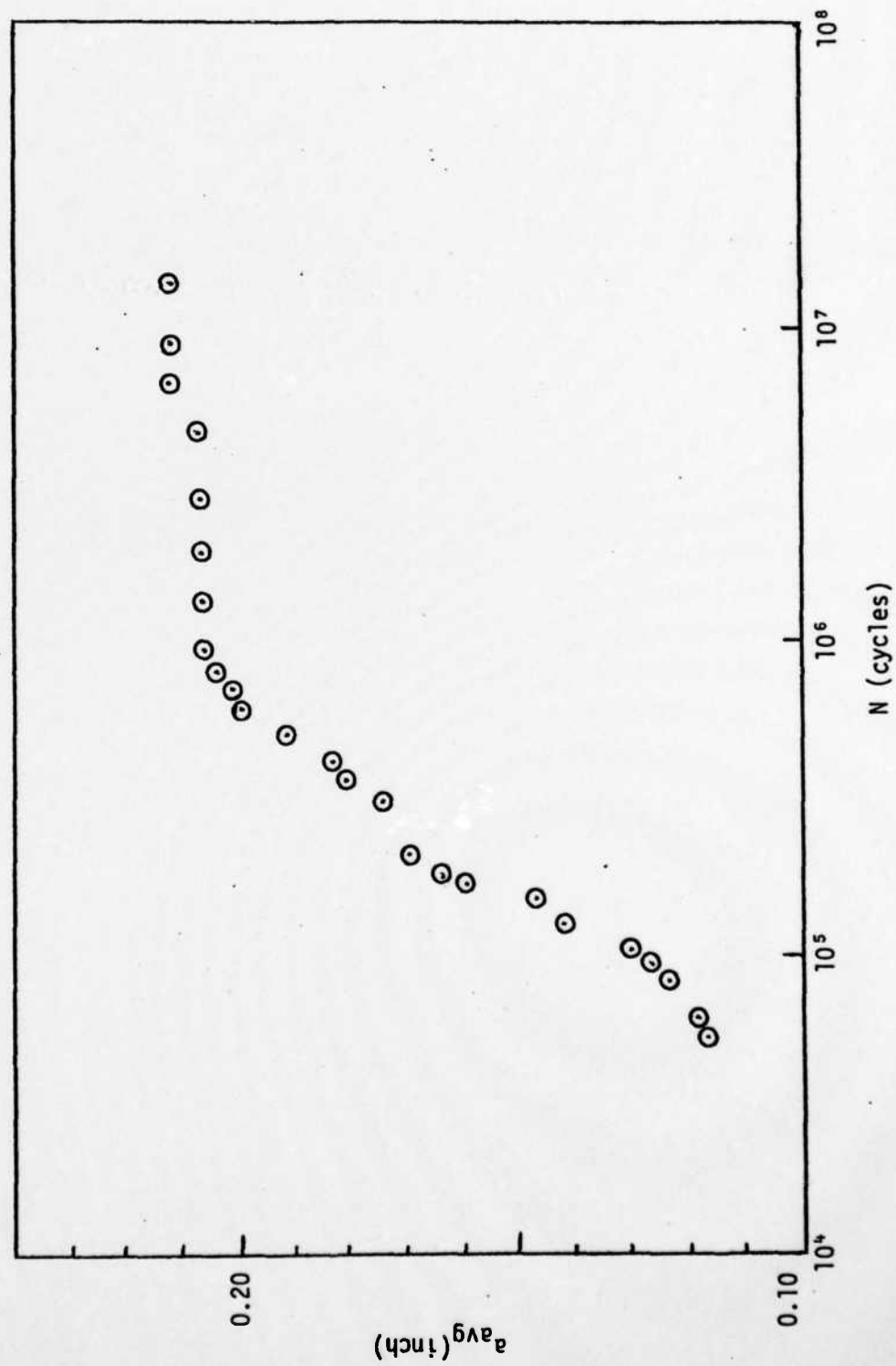


Figure 28. Average Crack Length Versus Number of Cycles for Specimen #10 (7175-T651 L-T, $R = 0.3$)

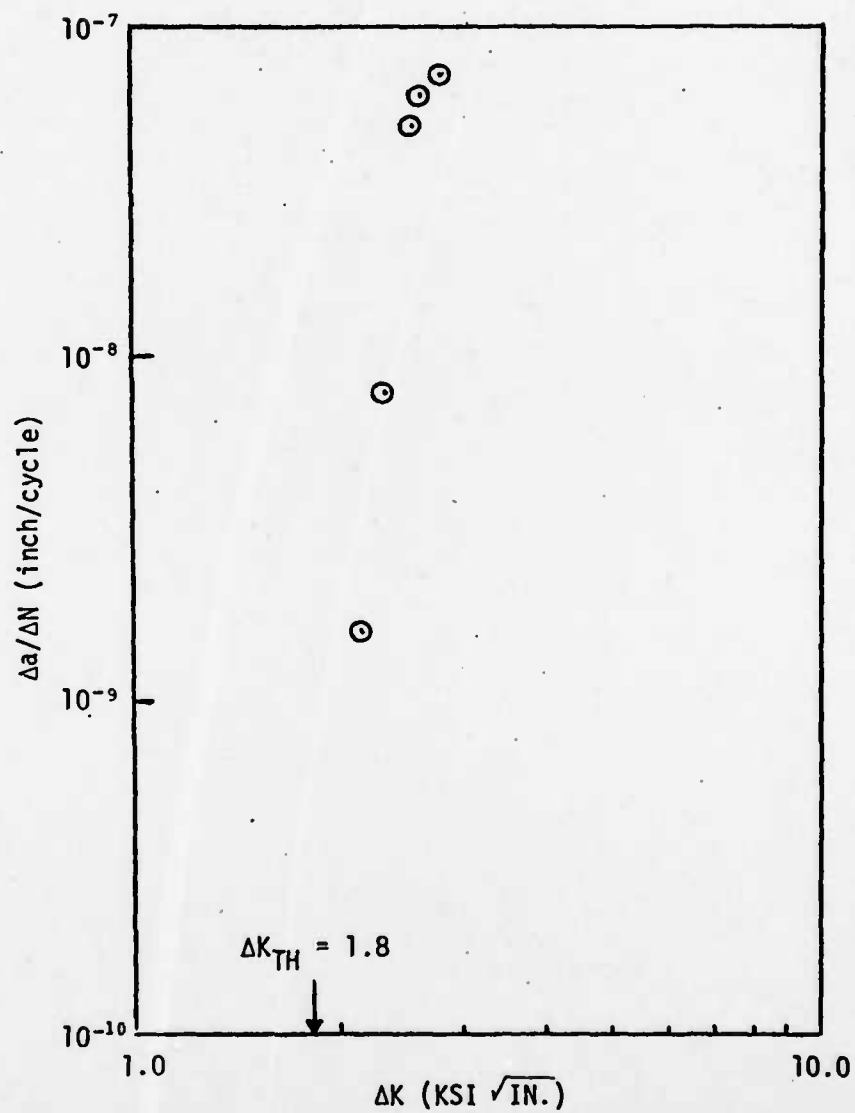


Figure 29. Fatigue Crack Growth Rate Versus Stress Intensity Factor Range for Specimen #10 (7175-T651 L-T, R = 0.3)

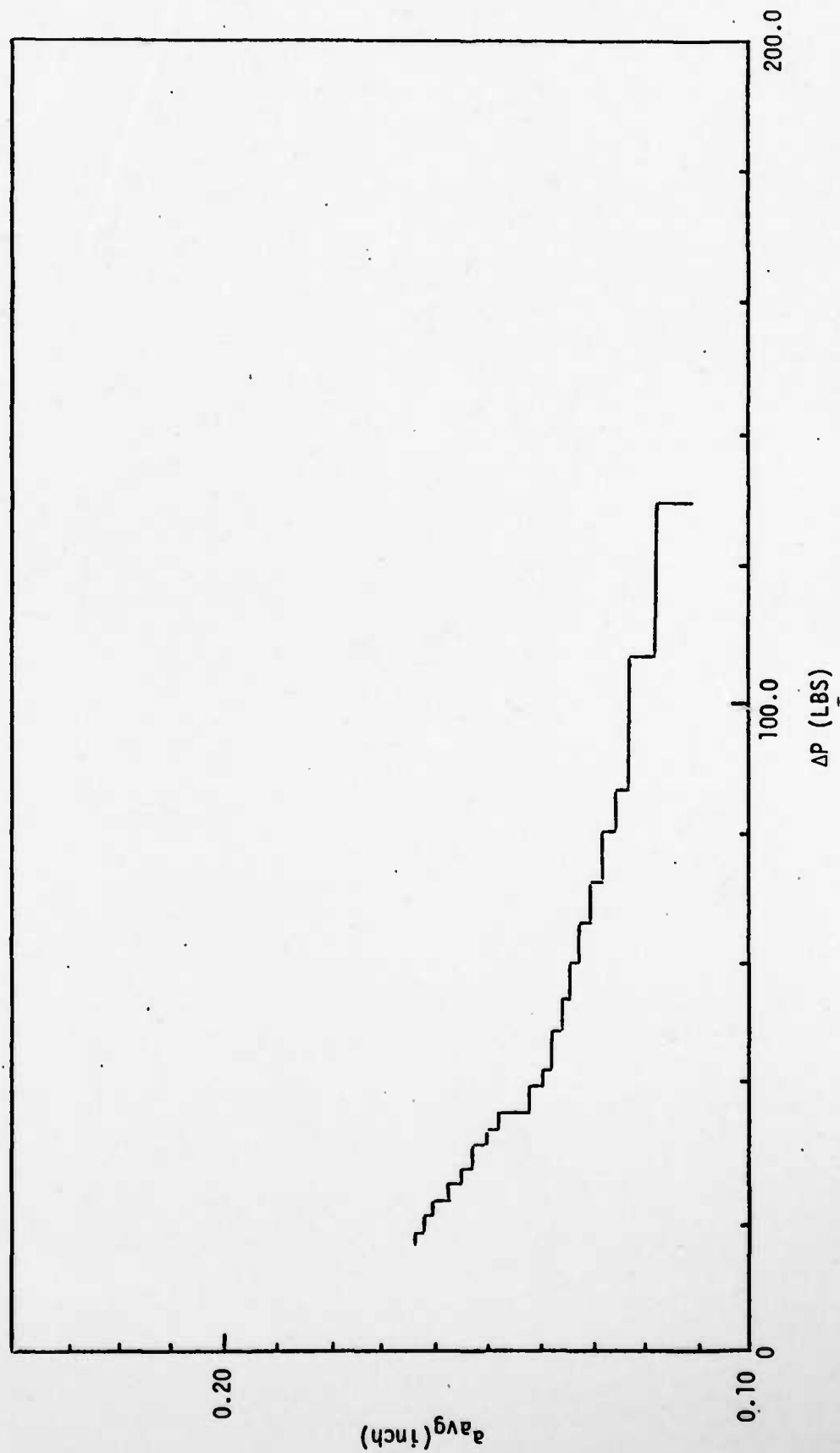


Figure 30. Average Crack Length Versus $\Delta P(\Delta P = P_{max} - P_{min})$ for Specimen #13 (MA-87 T-L, $R = 0.1$)

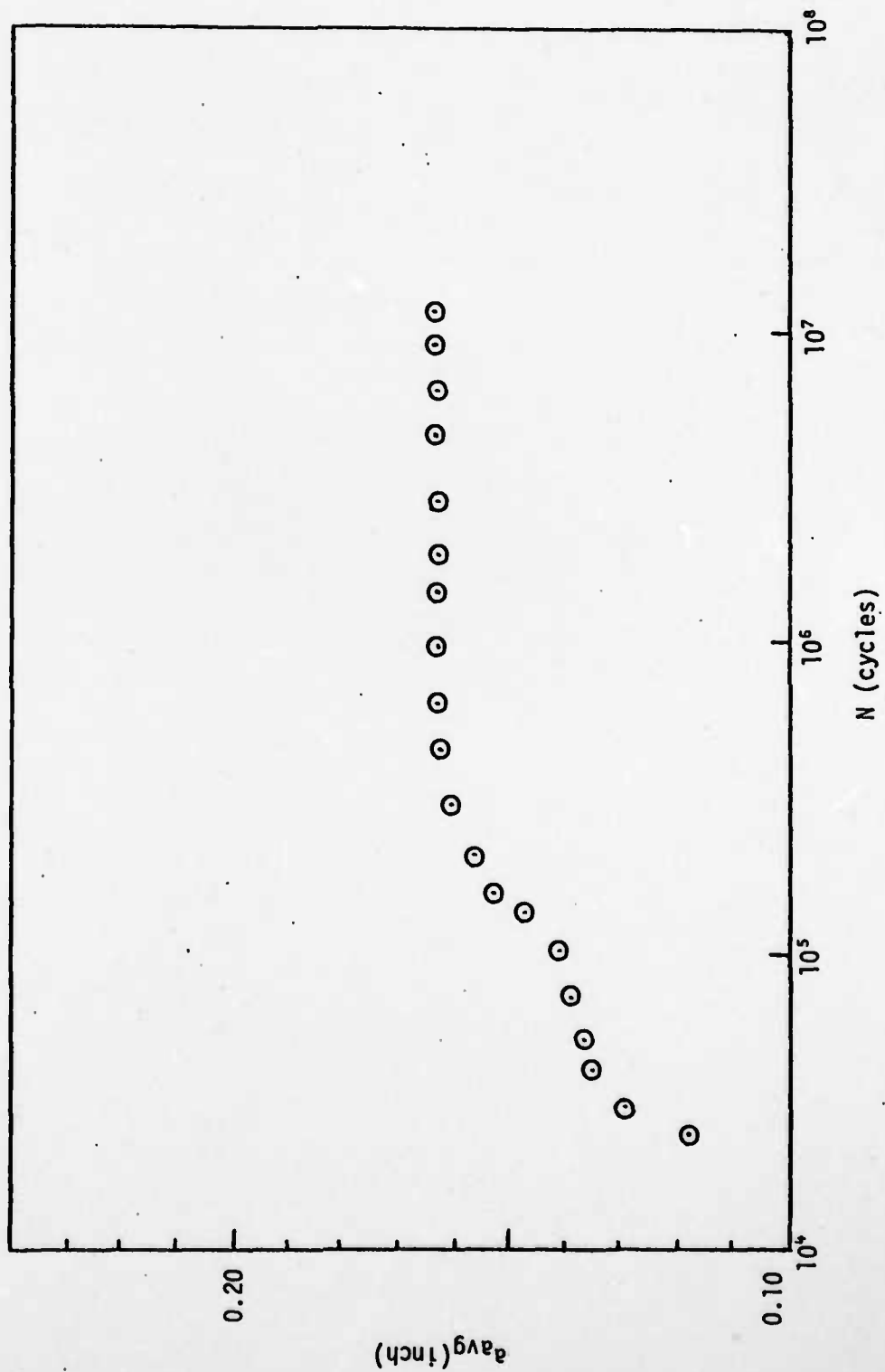


Figure 31. Average Crack Length Versus Number of Cycles for Specimen #13 (MA-87 T-L, $R = 0.1$)

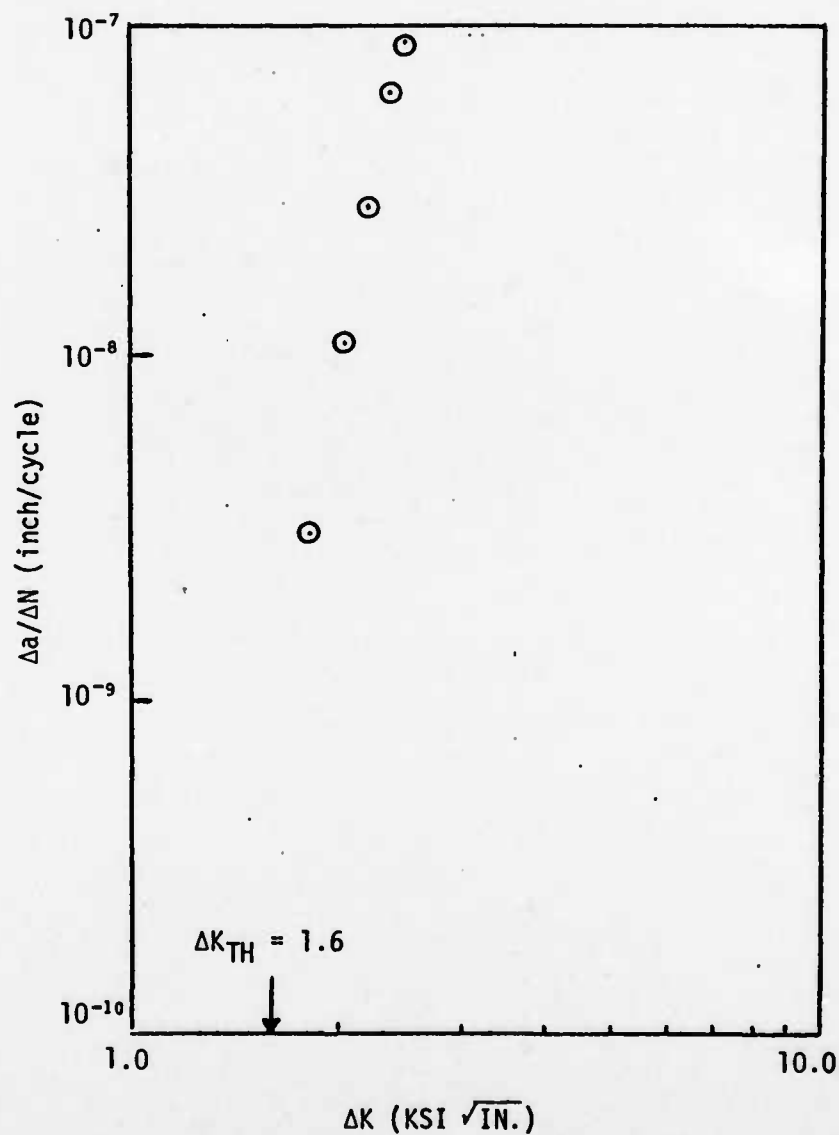


Figure 32. Fatigue Crack Growth Rate Versus Stress Intensity Factor Range for Specimen #13 (MA-87 T-L, R = 0.1)

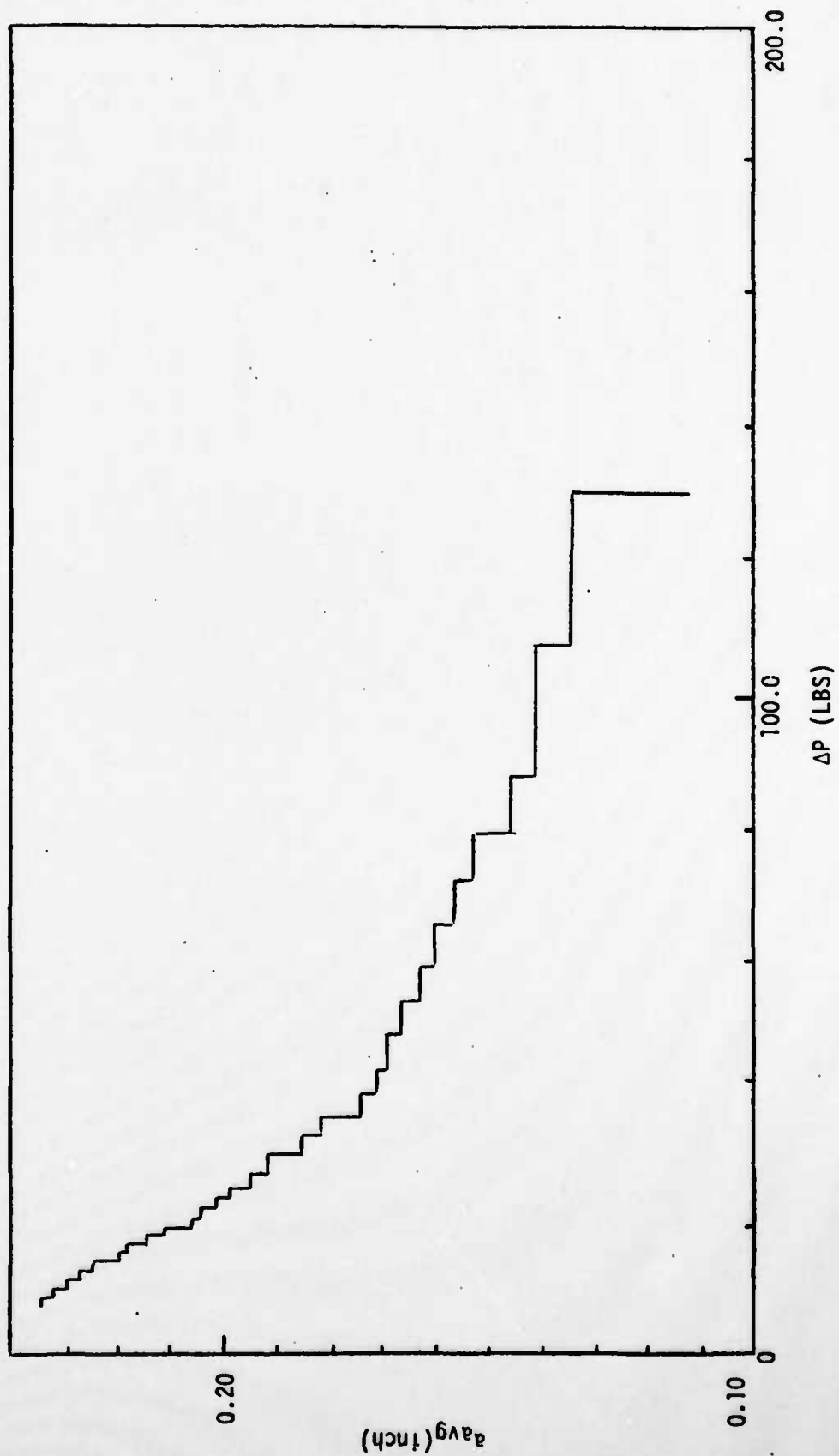


Figure 33. Average Crack Length Versus $\Delta P(\Delta P = P_{max} - P_{min})$ for Specimen #15 (MA-87 T-L, $R = 0.1$)

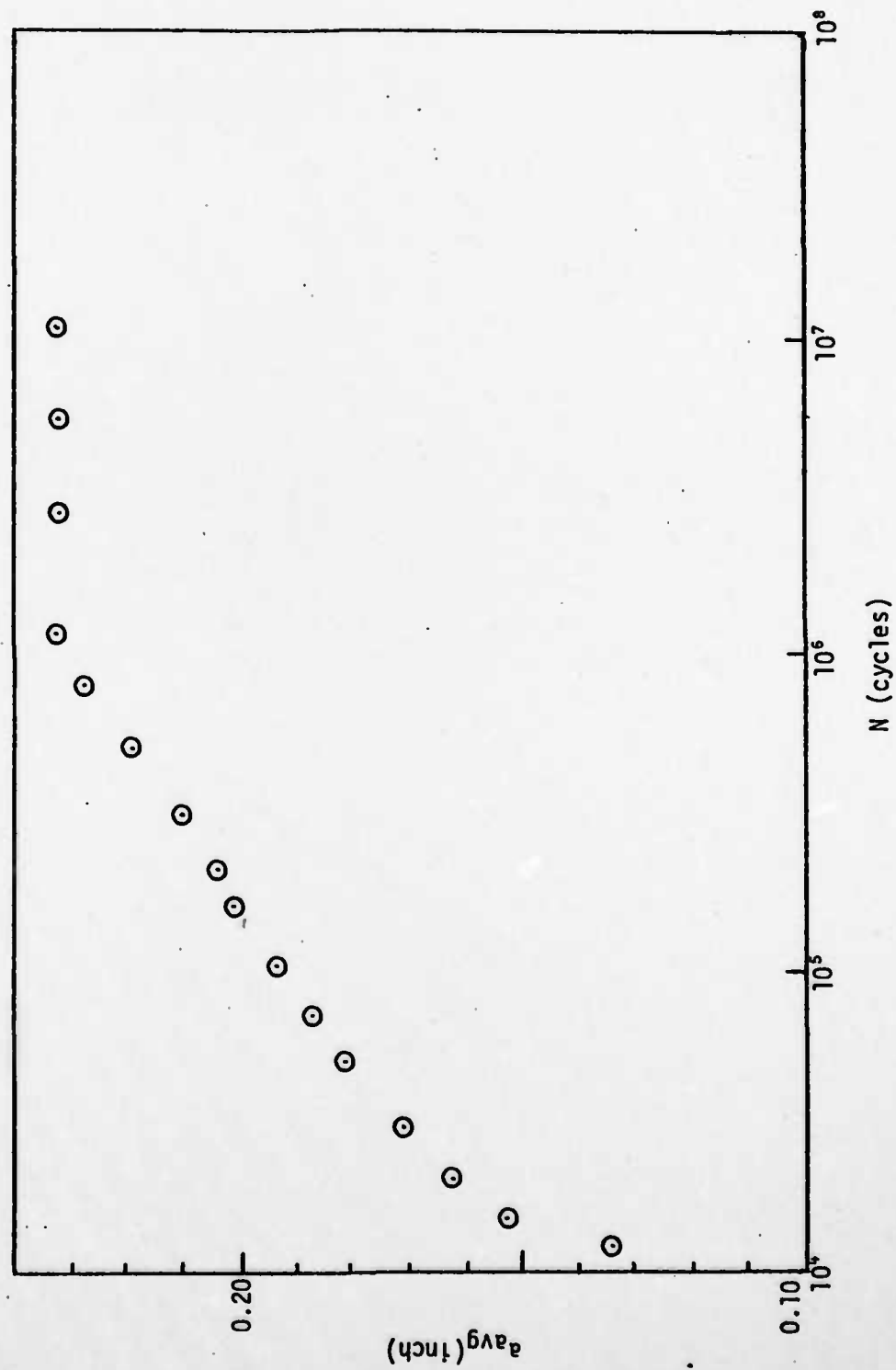


Figure 34. Average Crack Length Versus Number of Cycles for Specimen #15 (MA-87 T-L, $R = 0.1$)

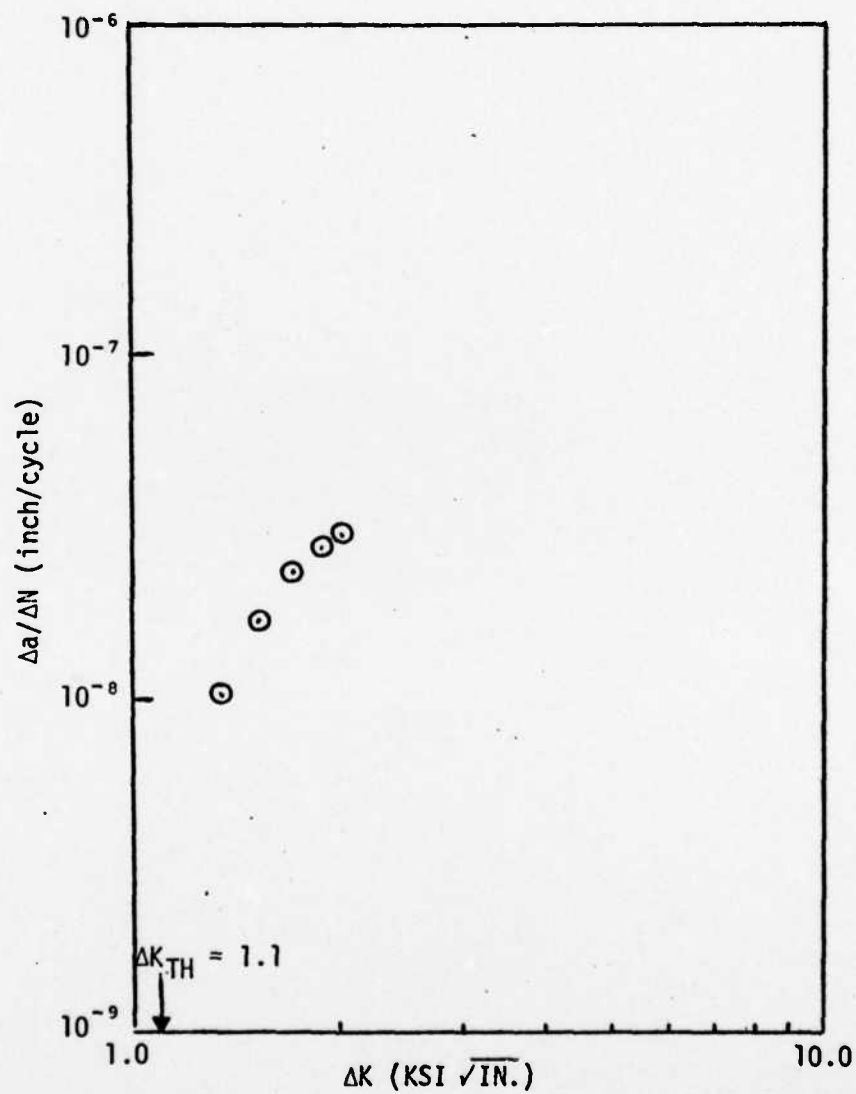


Figure 35. Fatigue Crack Growth Rate Versus Stress Intensity Factor Range for Specimen #15 (MA-87 T-L, R = 0.1)

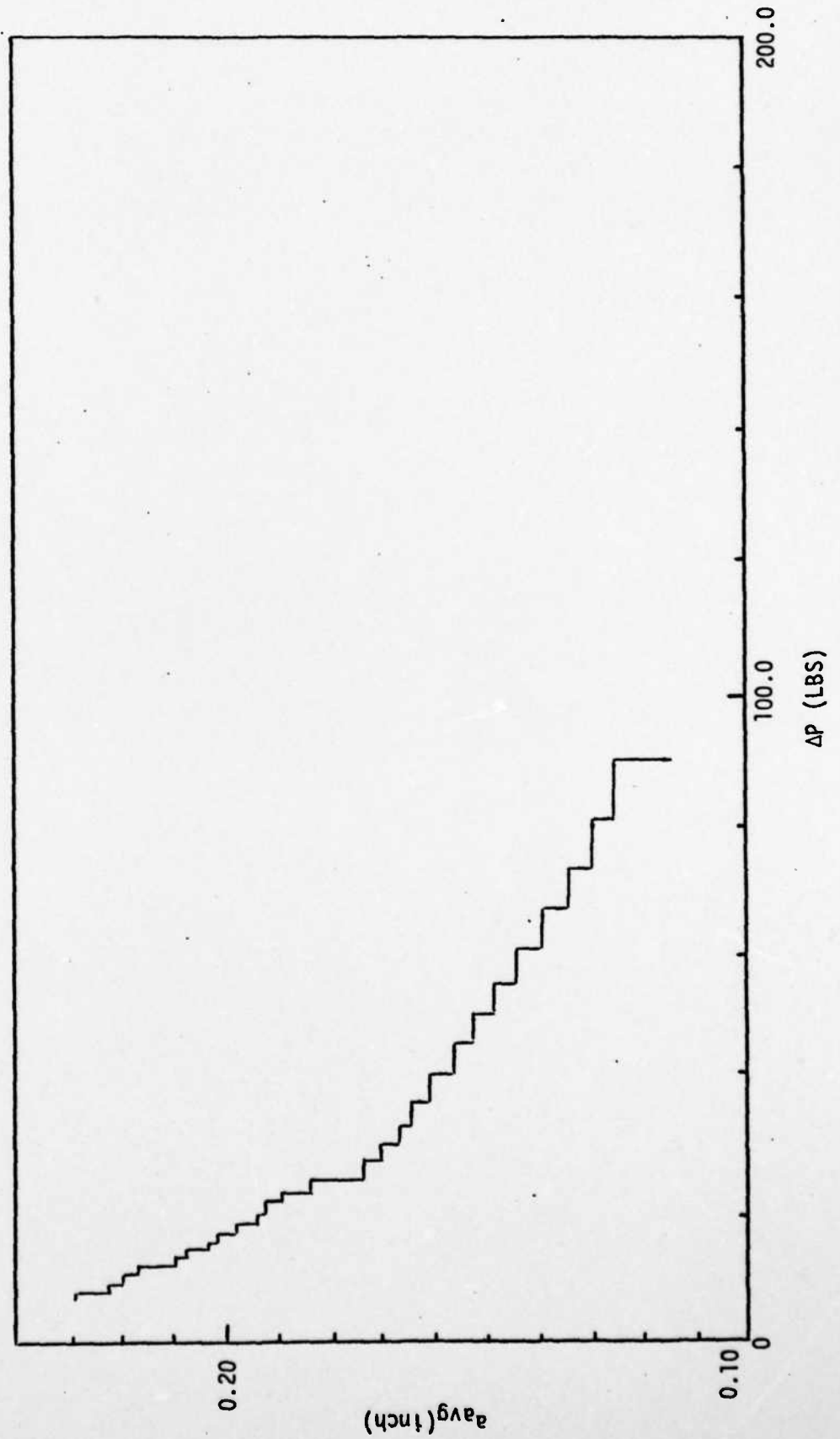


Figure 36. Average Crack Length Versus ΔP ($\Delta P = P_{max} - P_{min}$) for Specimen #16(MA-87 T-L, $R = 0.3$)

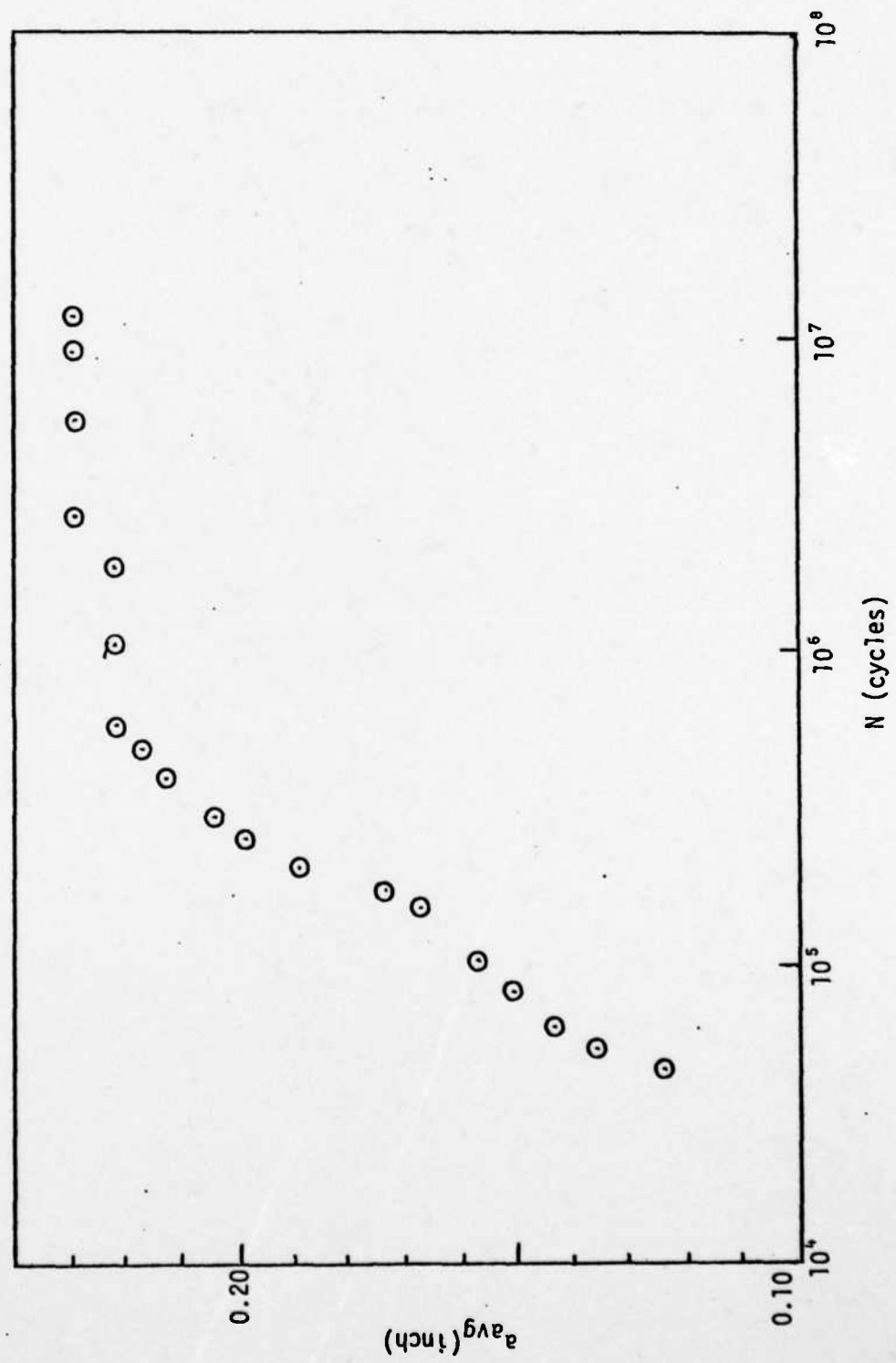


Figure 37. Average Crack Length Versus Number of Cycles for Specimen #16 (MA-87 T-L, $R = 0.3$)

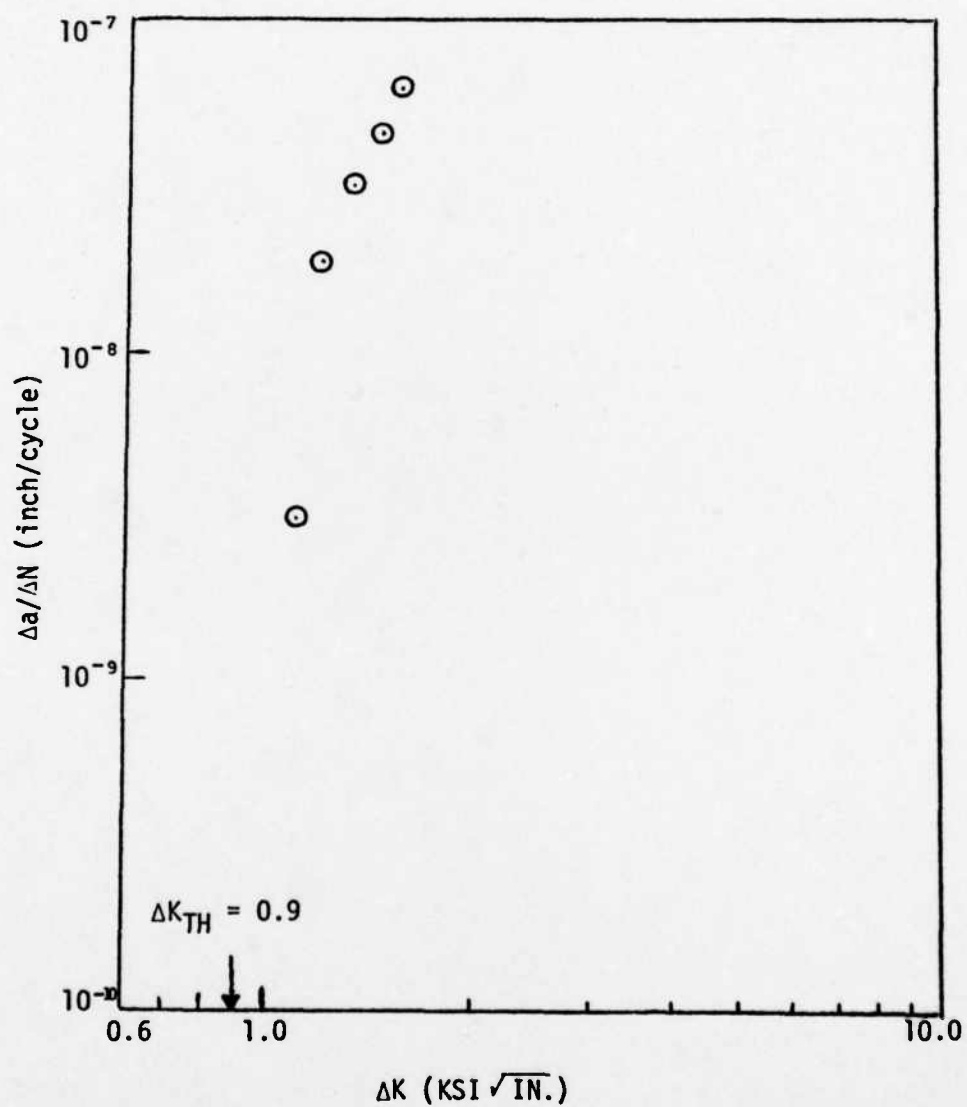


Figure 38. Fatigue Crack Growth Rate Versus Stress Intensity Factor Range for Specimen #16 (MA-87 T-L, R = 0.3)

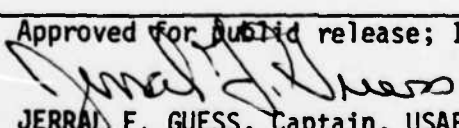
VITA

Donald Roy Holloway was born on 4 December 1946 in Americus, Georgia. He graduated from high school in Blakely, Georgia in 1964 and attended Georgia Southwestern College and Auburn University from which he received the degree of Bachelor of Aerospace Engineering in June 1969. Upon graduation, he was employed in the accident investigation department for the McDonnell Douglas Corporation in St. Louis, Missouri until entering the Air Force in November 1969. He received a commission in the United States Air Force through the Officer Training School (OTS) program, completed pilot training, and received his wings in February 1970. He served as a C-47 Flight Check Pilot in the 1867th Facility Checking Squadron, Clark Air Base, Philippines, and then a B-52 co-pilot in the 34th Bomb Squadron, Wright-Patterson Air Force Base, Ohio until June 1975 when he entered the School of Engineering, Air Force Institute of Technology.

Permanent Address: 411 Barton St.
Blakely, Georgia 31723

UNCLASSIFIED

SECURITY CLASSIFICATION OF THIS PAGE (When Data Entered)

REPORT DOCUMENTATION PAGE		READ INSTRUCTIONS BEFORE COMPLETING FORM
1. REPORT NUMBER AFIT/GAE/MC/77S-1	2. GOVT ACCESSION NO.	3. RECIPIENT'S CATALOG NUMBER
4. TITLE (and Subtitle) DETERMINATION OF THRESHOLD STRESS INTENSITY FACTORS FOR 7175-T651 ALUMINUM AND ALCOA MA-87 POWDERED ALUMINUM ALLOYS		5. TYPE OF REPORT & PERIOD COVERED MS Thesis
7. AUTHOR(s) Donald R. Holloway Captain USAF		6. PERFORMING ORG. REPORT NUMBER
9. PERFORMING ORGANIZATION NAME AND ADDRESS Air Force Institute of Technology (AFIT/EN) Wright-Patterson AFB, OH 45433		8. CONTRACT OR GRANT NUMBER(s)
11. CONTROLLING OFFICE NAME AND ADDRESS Metals Behavior Branch (AFML-LLN) Air Force Materials Laboratory Wright-Patterson AFB, OH 45433		10. PROGRAM ELEMENT, PROJECT, TASK AREA & WORK UNIT NUMBERS Project 2307-P102
14. MONITORING AGENCY NAME & ADDRESS (if different from Controlling Office)		12. REPORT DATE September 1977
		13. NUMBER OF PAGES 67
		15. SECURITY CLASS. (of this report) UNCLASSIFIED
		15a. DECLASSIFICATION/DOWNGRADING SCHEDULE
16. DISTRIBUTION STATEMENT (of this Report) Approved for public release; distribution unlimited.		
17. DISTRIBUTION STATEMENT (of the abstract entered in Block 20, if different from Report)		
18. SUPPLEMENTARY NOTES Approved for public release; IAW AFR 190-17  JERRAL F. GUESS, Captain, USAF Director of Information		
19. KEY WORDS (Continue on reverse side if necessary and identify by block number) Threshold stress intensity factors Fatigue crack growth Fracture mechanics 7175-T651 Aluminum Alcoa MA-87 Aluminum		
20. ABSTRACT (Continue on reverse side if necessary and identify by block number) Threshold stress intensity factors were obtained for two aluminum alloys: 7175-T651 and Alcoa MA-87, a powdered alloy. Crack growth tests were conducted at room temperature on a Sonntag Universal fatigue testing machine. Edge-cracked bent specimens were used in the tests. Crack length was checked periodically using a Gaertner cathetometer coupled with an auxillary lens placed close to the specimen. Tests were performed at stress ratios of R=0.1 and R=0.3. It was found that 7175-T651 had a greater fatigue threshold value than MA-87 when compared at the same stress ratio. It was also found that stress ratio had an		

DD FORM 1473
1 JAN 73

EDITION OF 1 NOV 65 IS OBSOLETE


UNCLASSIFIED

SECURITY CLASSIFICATION OF THIS PAGE (When Data Entered)

UNCLASSIFIED

SECURITY CLASSIFICATION OF THIS PAGE(When Data Entered)

effect on the threshold stress intensity factors with increasing stress ratio resulting in a smaller fatigue threshold value. Recommendations have been made for further experimentation with regard to threshold stress intensity factors of powdered aluminum alloys.



UNCLASSIFIED

SECURITY CLASSIFICATION OF THIS PAGE(When Data Entered)

**DAT
FILM**